A scenario-based distributed model predictive control approach for freeway networks

Liu, Shuai; Sadowska, Anna; De Schutter, Bart

DOI
10.1016/j.trc.2021.103261

Publication date
2022

Document Version
Final published version

Published in
Transportation Research Part C: Emerging Technologies

Citation (APA)
Liu, S., Sadowska, A., & De Schutter, B. (2022). A scenario-based distributed model predictive control approach for freeway networks. *Transportation Research Part C: Emerging Technologies*, *136*, Article 103261. https://doi.org/10.1016/j.trc.2021.103261

Transportation Research Part C 136 (2022) 103261

Contents lists available at ScienceDirect

Transportation Research Part C

journal homepage: www.elsevier.com/locate/trc

A scenario-based distributed model predictive control approach for freeway networks☆

Shuai Liu [a,*], Anna Sadowska [b], Bart De Schutter [c]

[a] The National Innovation Institute of Defense Technology, Beijing, China
[b] The Schlumberger Cambridge Research, Cambridge, United Kingdom
[c] The head of the Delft Center for Systems and Control, Delft University of Technology, Delft, the Netherlands

ARTICLE INFO

Keywords:
Scenario-based DMPC
Reduced scenario tree
Global and local uncertainties
Freeway networks

ABSTRACT

In this paper a scenario-based Distributed Model Predictive Control (DMPC) approach based on a reduced scenario tree is developed for large-scale freeway networks. In the new scenario-based DMPC approach, uncertainties in a large-scale freeway network are distinguished into two categories: global uncertainties for the overall network and local uncertainties applicable to subnetworks only. We propose to use a reduced scenario tree instead of using a complete scenario tree. A complete scenario tree is defined as a scenario tree consisting of global scenarios and all the combinations of the local scenarios for all subnetworks, while a reduced scenario tree is defined as a scenario tree consisting of global scenarios and a reduced local scenario tree in which local scenarios are combined within each subnetwork, not among subnetworks. Moreover, an expected-value setting and a min–max setting are considered for handling uncertainties in scenario-based DMPC. In the expected-value setting, the expected-value of the cost function values for all considered uncertainty scenarios is optimized by scenario-based DMPC. However, in the min–max setting, the worst-case of the cost function values for all considered uncertainty scenarios is optimized by scenario-based DMPC. The results for a numerical experiment show that the new scenario-based DMPC approach is effective in improving the control performance while at the same time satisfying the queue constraints in the presence of uncertainties. Additionally, the proposed approach results in a relatively low computational burden compared to the case with the complete scenario tree.

1. Introduction

With the development of modern society, traffic congestion has become a common phenomenon that people experience in daily life. Traffic congestion can result in a waste of time and energy, a high risk of traffic accidents, with detrimental effects on both mental and physical health of drivers. Since improving and extending traffic infrastructure is difficult and expensive, researchers have been making efforts on relieving traffic jam by means of traffic management. Traffic control is an important measure to realize dynamically traffic management. Typical traffic control approaches include fuzzy control (Hoyer and Jumar, 1994; Precup and Hellendoorn, 2011), neural network control (Srinivasan et al., 2006; Kato et al., 2017), adaptive control (Zheng and Recker, 2013; Haddad and Mirkin,

☆ The research is supported by the China Scholarship Council, and National Natural Science Foundation of China (61790565).
* Corresponding author.
E-mail addresses: shuailiu_tud@163.com (S. Liu), ASadowska@slb.com (A. Sadowska), b.deschutter@tudelft.nl (B. De Schutter).

https://doi.org/10.1016/j.trc.2021.103261
Received 2 September 2020; Received in revised form 13 May 2021; Accepted 7 June 2021
Available online 11 January 2022

2016), etc. Model Predictive Control (MPC) for traffic networks has also been receiving more and more attention in the literature (Hegyi et al., 2005; Papamichail et al., 2010; Ferrara et al., 2015; Luo et al., 2016; Kim et al., 2017; Piacentini et al., 2018; Menelaou et al., 2019; Sirmatel and Geroliminis, 2018; Maestre et al., 2020). In this paper, our research is mainly about the control problem for freeway networks. However, in this section, some control approaches for urban traffic networks are also included, considering that they can probably be extended for freeway networks. The motivation for this paper is to develop a control scheme to reduce traffic congestion caused by heavy traffic demand in large-scale freeway networks, with uncertainties being considered.

In MPC for traffic networks, macroscopic traffic models are often used for predicting the future evolutions of the controlled traffic networks. Since the predictions of the future evolutions of the controlled networks are used for determining the optimal control actions in MPC, the uncertainties that affect the accuracy of the predictions will also affect the control performance and the satisfaction of constraints on states and outputs. In particular, these uncertainties include the uncertainties in the measurements of states, the uncertainties in the model parameters, the uncertainties in the external uncontrollable inputs, and so on. There are some approaches available in the literature for handling uncertainties for MPC. Tettamanti et al. (2014) developed a robust MPC approach based on a min–max scheme and a linear model for urban networks, with constraints defined for all possible uncertainties. For nonlinear systems, one kind of approach is based on Lyapunov functions, see e.g. (Scokaert et al., 1997; De Nicolao et al., 1998). Another kind of approach is tube-based MPC, see e.g. (Mayne et al., 2011), where a model predictive controller forces the trajectories of the disturbed system to be within a tube around a central reference trajectory, which is obtained by a nominal control approach with tightened constraints on states and inputs. Moreover, a min–max scheme is used for handling uncertainties in (Campo and Morari, 1987; Gruber et al., 2013), where the worst-case control objective functions for all the considered uncertainties are optimized. In (Campo and Morari, 1987) constraints on control inputs and system outputs are defined for all possible uncertainties, and in (Gruber et al., 2013) only constraints on control inputs are considered. In (Liu et al., 2016), Liu et al. have developed a centralized robust predictive control approach for freeway networks based on a min–max scheme with constraints on queue lengths included in the control objective function as a penalty term.

A large-scale traffic network is hard to control by centralized MPC due to the computational complexity. In Distributed Model Predictive Control (DMPC), a large-scale network is divided into smaller subnetworks, which are assigned to local controllers. Accordingly, the overall optimization problem is decomposed into local optimization problems for the local controllers by methods such as primal decomposition or dual decomposition (Christofides et al., 2013). In the dual decomposition method (Christofides et al., 2013; Negenborn et al., 2008), coupling constraints among subnetworks are incorporated into the overall control objective function by Lagrangian relaxation or augmented Lagrangian relaxation, resulting in a dual problem that can be decomposed into local optimization problems. It can be shown (Negenborn et al., 2008; Camponogara et al., 2002; Bertsekas, 1982) that when the control objective functions and the inequality constraints of subnetworks are convex and the equality constraints of subnetworks are affine, the solution of the original overall optimization problem can be retrieved by iteratively solving the dual problem with Lagrange multipliers fixed within one iteration, and for the current iteration the Lagrange multipliers are computed based on the solution for the previous iteration. Some researchers also use DMPC for nonlinear-nonconvex systems, and they use numerical experiments for investigating the control effectiveness. For instance, Frejo and Camacho applied DMPC for a nonlinear-nonconvex freeway network in (Frejo and Camacho, 2012), where they did not include coupling terms in the control objective function, and they adopted a setting in which each local controller can negotiate with other controllers through communication about coupling variables. Frejo and Camacho (2012) showed by a numerical experiment that DMPC can improve the control performance w.r.t. the no-control case, albeit that the control performance is suboptimal compared to that for the centralized control approach. Ferrara et al. (2015) reformulated a nonlinear traffic flow model as a mixed logical dynamical system including linear equalities and inequalities. By considering a freeway network as a system of systems, Ferrara et al. (2015) developed two different DMPC approaches: a so-called partially connected noniterative independent algorithm where each local controller optimizes a local control objective function, and a so-called partially connected noniterative cooperative algorithm where each local controller optimizes the weighted sum of the control objective functions of that local controller and all neighbors. Ferrara et al. (2015) showed by a case study that the control performance can be improved by DMPC compared to the no-control case, and that the DMPC approach based on the so-called partially connected noniterative cooperative algorithm leads to a control performance that is close to that for the centralized control approach.

In DMPC, local controllers communicate with other controllers to obtain solutions in a cooperative way for the control problem of the overall network (Maestre and Negenborn, 2014). Therefore, apart from the uncertainties of the current local controller, the uncertainties appearing in other local controllers also affect the control effectiveness of DMPC. Some robust DMPC approaches have been developed in (Richards and How, 2007; Giselsson, 2013; Li and Shi, 2014; Maestre et al., 2012; Martí et al., 2015; Leidereiter et al., 2015). More specifically, in (Richards and How, 2007; Giselsson, 2013) a constraint tightening scheme is used for dealing with uncertainties in DMPC for linear systems. In (Richards and How, 2007), constraints are tightened in a monotonic way to ensure robust feasibility, including additional margins in the coupling constraints of each local controller to account for the uncertainties for neighboring subsystems. In (Giselsson, 2013), local constraint sets are tightened to account for uncertainties, and the global constraint set is taken as the Cartesian product of tightened local constraint sets, ensuring robustness w.r.t. small disturbances. For nonlinear systems, some robust DMPC approaches are also available in the literature. Li and Shi (2014) proposed a robust DMPC approach for continuous-time decoupled nonlinear subsystems, where coupling occurring in a global control objective function is incorporated into local control objective functions. Particularly, a robustness constraint making local cost functions (Lyapunov functions) decrease was proposed to ensure robustness against external bounded disturbances. For robust control design, the scenario approach with a finite number of uncertainty scenarios considered was proposed by Calafiore and Campi (2006) for control problems with linear objective functions and convex constraints. Calafiore and Campi (2006) established a bound on the number of uncertainty scenarios needed for achieving a specified probabilistic robustness level, which is defined as an upper bound of the probability of violation of constraints;

moreover, they showed that the bound only increases slowly with the increase of the specified probabilistic robustness level. The scenario approach is an efficient way for reducing the computational complexity in robust control problems. In addition, further analyses and applications of the scenario-based scheme can be found in (Bernardini and Bemporad, December 2009; Calafiore and Fagiano, 2013; Zhang et al., 2013; Schildbach et al., 2014). Furthermore, some robust DMPC approaches have been developed for nonlinear systems based on scenario trees for uncertainties (Maestre et al., 2012; Martí et al., 2015; Leidereiter et al., 2015). In these approaches, the considered scenarios for uncertainties are distributed to different local controllers, i.e. each local controller deals with one scenario for uncertainties. Non-anticipativity constraints, which are incorporated into local control objective functions, are introduced in these approaches for ensuring that the control inputs of one controller equal the control inputs of other controllers at the same time step. Note, however, that the approaches in (Maestre et al., 2012; Martí et al., 2015; Leidereiter et al., 2015) are not for multiple subsystems, but for a single system only. The authors have developed scenario-based DMPC for freeway networks for multiple subnetworks by considering a min–max setting in (Liu et al., 2016).

In this paper, we develop a scenario-based DMPC approach for a large-scale freeway network including multiple subnetworks based on a scenario tree for uncertainties. Although centralized linear MPC approaches have been studied in the literature (Le et al., 2013; Han et al., 2017), the inherent nonlinearity of freeway networks cannot be ignored. Thus, in this paper we consider nonlinear traffic flow models for prediction. Our aim is to develop an approach based on distributed nonlinear MPC to deal with large-scale network control with uncertainties being directly handled. For a large-scale freeway network consisting of multiple subnetworks, we propose a novel way of dealing with uncertainties and consequently distinguish two types of uncertainties: global and local. The global uncertainties apply to the overall network, while the local uncertainties only apply to a single subnetwork. We assume that all these uncertainties are described by means of finite sets of scenarios. An intuitive way of combining the local scenarios for different subnetworks is to consider all the combinations of the local scenarios (i.e. to construct a complete local scenario tree). However, the computational burden will be very large in this case. Therefore, we propose a new approach for combining the local scenarios for different subnetworks: *we construct a reduced local scenario tree*. In the reduced local scenario tree, the dynamics of a subnetwork are predicted for different local scenarios for that subnetwork, by assuming that the interconnecting inputs for that subnetwork from neighbors are independent of the local scenarios for the neighbors. In fact, the interconnecting inputs for a subnetwork and the interconnecting outputs from the neighbors to that subnetwork correspond to the same physical quantities. Thus the interconnecting outputs are combined for all the local scenarios for a neighbor to obtain the combined interconnecting outputs independent of the local scenarios for that neighbor. Afterwards, a reduced scenario tree for the entire network can be defined by combining global scenarios with the reduced local scenario tree. Readers can refer to Section 4.1.2 for more details about the scheme of the complete scenario tree and the reduced scenario tree. In order to handle uncertainties in the scenario-based control problem, we consider an expected-value setting (which is probabilistic) and a min–max setting for combining local scenarios for each subnetwork and for defining objective functions that include both performance indicators and constraint violation penalties for subnetworks.

The newly proposed scenario-based DMPC approach in this paper is developed based on the dual decomposition method and the augmented Lagrangian relaxation method. As an illustration, the Alternating Direction Method of Multipliers (ADMM) (Boyd et al.,

Table 1
Main quantities in METANET.

T	simulation time step length
k	simulation time step counter
m	index for links
i	index for segments
o	index for origins, on-ramps or off-ramps
μ_m	number of lanes in link m
L_m	length of segments of link m
$q_{m,i}(k)$	flow for segment (m,i)
$\rho_{m,i}(k)$	density for segment (m,i)
$v_{m,i}(k)$	speed for segment (m,i)
$q_o(k)$	flow for origin, on-ramp or off-ramp o
$w_o(k)$	queue length for origin, on-ramp or off-ramp o
C_o	capacity for origin, on-ramp or off-ramp o
$d_o(k)$	demand for origin or on-ramp o
$r_o(k)$	metering rate for on-ramp o
$v_{m,i}^{\mathrm{SL}}(k)$	speed limit for segment (m,i)
v_m^{free}	free flow speed in link m
ρ_m^{crit}	critical density in link m
$\rho_m^{\max}$	maximum density in link m
δ_m	$1+\delta_m$: compliance factor in link m
τ	model parameter in the dynamic equation for $v_{m,i}$
η	model parameter in the dynamic equation for $v_{m,i}$
κ	model parameter in the dynamic equation for $v_{m,i}$
a_m	model parameter in the dynamic equation for $v_{m,i}$

2011) is chosen as the DMPC algorithm in this paper. Note that the newly proposed scenario-based DMPC approach is independent of the considered DMPC algorithm, and it can be easily combined with other DMPC algorithms based on the dual decomposition method, such as the serial DMPC algorithm proposed in (Negenborn et al., 2008), the inexact dual fast gradient method in (Maestre and Negenborn, 2014), accelerated gradient methods (Giselsson et al., 2013), etc.

The paper is organized as follows. In Section 2, we introduce model predictive control for freeway networks. In Section 3, we present general DMPC based on dual decomposition. In Section 4.1, we describe how to distinguish global uncertainties for the overall network with local uncertainties for subnetworks, and we develop a reduced scenario tree of global and local uncertainties. In Section 4.2, we propose a new scenario-based DMPC approach based on global uncertainties and local uncertainties. In Section 5, ADMM is applied to the new scenario-based DMPC approach. After that, a case study is reported in Section 6 to show the efficiency of the new scenario-based DMPC approach. At last, we give the conclusions of this paper and some recommendations for future work.

2. Model Predictive Control for Freeway Networks

In Model Predictive Control (MPC) (Maciejowski, 2002; Camacho and Bordons, 2007) for traffic networks, macroscopic traffic models are used for predicting the performance of the considered traffic network over the prediction period. For a control step, the predicted future performance is optimized, resulting in a sequence of control inputs over the control period, of which the first element is applied to the controlled network. After that, for the next control step, the prediction period is shifted one control step ahead according to the receding-horizon scheme.

As an illustration, we use METANET (Messmer and Papageorgiou, 1990; Kotsialos et al., 2002) as the prediction model for MPC; however, other traffic models (e.g. the Cell Transmission Model (CTM) (Daganzo, 1995)) can be also used. METANET is a second-order macroscopic model for describing traffic flows. In METANET, freeway stretches are represented by links that are considered to have uniform characteristics within each link. Each link is divided into segments, of which the dynamics are described by flows, densities, and speeds. Once there is a major change in geometry, an on-ramp, or an off-ramp between two freeway stretches, a node will be placed between the corresponding links. For this node, there could be one or more incoming links and one or more leaving links. For incoming links a downstream density is provided by this node, and for leaving links an inflow and an upstream speed are provided by this node. We list the main variables of METANET in Table 1. We refer to (Messmer and Papageorgiou, 1990; Kotsialos et al., 2002; Hegyi et al., 2005) for more details about METANET and its extensions, e.g. link equations and node equations.

Typical traffic control measures for freeway networks include ramp metering, variable speed limits, route guidance, etc. Ramp metering determines the rate at which vehicles in a ramp can enter the main freeway. Variable speed limits are used for adapting speeds of vehicles according to traffic situations. Route guidance is used for choosing an appropriate route when more than one routes exist to a certain destination. In this paper, we choose ramp metering and variable speed limits as the control measures in the case study. The desired speed equation including a variable speed limit in segment i of link m can be defined as follows (Hegyi et al., 2005):

$$V\left(\rho_{m,i}\left(k\right)\right) = \min\left(v_m^{\text{free}}\exp\left(-\frac{1}{a_m}\left(\frac{\rho_{m,i}\left(k\right)}{\rho_m^{\text{crit}}}\right)^{a_m}\right), \left(1+\delta_m\right)v_{m,i}^{\text{SL}}\left(k\right)\right) \tag{1}$$

The first term on the right-hand side of (1) refers to the desired speed according to the fundamental diagram, while the second term reflects the variable speed limit including a non-compliance factor. The flow for an on-ramp origin o that connects to link m is described as

$$q_o\left(k\right) = \min\left[d_o\left(k\right) + \frac{w_o(k)}{T}, C_o r_o\left(k\right), C_o\left(\frac{\rho_m^{\max} - \rho_{m,1}\left(k\right)}{\rho_m^{\max} - \rho_m^{\text{crit}}}\right)\right] \tag{2}$$

The first term on the right-hand side of (2) refers to the total available traffic demand at o, the second term refers to the maximal flow allowed by the ramp metering rate, and the third term reflects the maximal flow allowed by the mainstream condition. Readers can refer to Table 1 for symbols in Eqs. (1) and (2).

We consider the Total Time Spent (TTS) as the main part of the performance criterion for MPC. The TTS is defined according to the total time that all vehicles spend in the considered traffic network (Hegyi et al., 2005). Note, however, that the Total Emissions (TE)[1] can also be dealt with by the approaches in this paper. In the following text, N_{p} represents the prediction horizon, i.e. the number of prediction control time steps, I_{all} is the set of all pairs of links and segments in the considered network, and O_{all} is the set of all origins in the considered network. According to (Hegyi et al., 2005), the TTS is defined as follows:

$$\text{TTS}\left(k\right) = T\sum_{z=k}^{k+N_{\text{p}}-1}\left(\sum_{(m,i)\in I_{\text{all}}}\rho_{m,i}\left(z\right)L_m\mu_m + \sum_{o\in O_{\text{all}}}w_o\left(z\right)\right) \tag{3}$$

Remark 1. Note that in general the simulation time step length T is not equal to the control time step length, but we assume that they are equal for simplifying notations while developing the newly proposed approaches in this paper.

[1] The total emissions for a traffic network can be estimated as the sum of the emission estimates of all vehicles in that traffic network; readers can refer to (Liu et al., 2017; Pasquale et al., 2017; Pasquale et al., 2019) for more details.

The control objective function for MPC depends on system states, control actions and outputs, and all these quantities depend on time steps. Thus we represent the objective function as $J(k)$ for simplification in this section. In the following text, N_c represents the control horizon, $\mathrm{TTS}_{\mathrm{nom}}$ is the TTS computed for some nominal case, $\xi_{\mathrm{TTS}}, \xi_{\mathrm{ramp}}$, and ξ_{speed} are nonnegative weights, O_{ramp} is the set of all the metered origins, I_{speed} is the set of all the segments with speed limits, N_{RM} is the number of the metered on-ramps, N_{VSL} is the number of variable speed limits, r_o^{ctrl} is the ramp metering rate for on-ramp o at a given control step, $v_{m,i}^{\mathrm{ctrl}}$ is the variable speed limit in segment i of link m at a given control step. Considering Variable Speed Limits (VSL) and Ramp Metering (RM) as control measures, the control objective function for MPC of the considered network can be defined as follows:

$$\begin{aligned} J\left(k\right) = \xi_{\mathrm{TTS}}\frac{\mathrm{TTS}(k)}{\mathrm{TTS}_{\mathrm{nom}}} + \frac{\xi_{\mathrm{ramp}}}{N_c N_{\mathrm{RM}}}\sum_{z=k}^{k+N_c-1}\sum_{o\in O_{\mathrm{ramp}}}\left\|r_o^{\mathrm{ctrl}}\left(z\right) - r_o^{\mathrm{ctrl}}\left(z-1\right)\right\|_2 \\ + \frac{\xi_{\mathrm{speed}}}{N_c N_{\mathrm{VSL}}}\sum_{z=k}^{k+N_c-1}\sum_{\left(m,i\right)\in I_{\mathrm{speed}}}\left\|\frac{v_{m,i}^{\mathrm{ctrl}}\left(z\right) - v_{m,i}^{\mathrm{ctrl}}\left(z-1\right)}{v_m^{\mathrm{free}}}\right\|_2 \end{aligned} \tag{4}$$

in which the second term and the third term are included for penalizing variations of the control inputs.

3. Distributed Model Predictive Control Based on Dual Decomposition

We consider a large-scale freeway network, which can be divided into several subnetworks. Couplings among subnetworks are described by means of interconnecting constraints for the subnetworks. The performance criteria are assumed to be additive for different subnetworks, i.e. the sum of the performance criteria for different subnetworks equals the performance criterion for the overall network. Note that in this paper, we directly present the formulation of a large network consisting of multiple subnetworks. Readers can refer to (Christofides et al., 2013; de Souza et al., 2014; Xie et al., 2016) for more details on decompositions of large-scale networks based on DMPC. In addition, we assume that all subnetworks include control measures. In fact, if a subnetwork does not include control measures, it is no need to assign a local controller for that subnetwork. Such a subnetwork without controllers should be merged with other subnetworks with control measures and thus with local controllers. The traffic state of that subnetwork will then be influenced by upstream and downstream traffic flows, which are determined by other local controllers.

Note that in the following part of this paper, k is the time step at which the control problem is solved. More specifically, s represents the index for a subnetwork, N_{sub} is the number of subnetworks, x_s represents the state vector of subnetwork s, x_s^k represents the measured state vector of subnetwork s at time step k, y_s represents the output vector of subnetwork s, u_s represents the control input vector for subnetwork s, J_s is the local control objective function of subnetwork s defined according to[2] (4), f_s is the dynamic function of subnetwork s, h_s is the output function of subnetwork s, S_s is the set of all the indices of the neighbors of subnetwork s, D_s^{in} represents the external uncontrollable input vector for subnetwork s (e.g. demands for subnetwork s), E_s^{in} is a stacked vector, representing the interconnecting input vector (w.r.t. local controller s) from all neighbors to subnetwork s, E_s^{out} is also a stacked vector, representing the interconnecting output vector (w.r.t. local controller s) from subnetwork s to all neighbors. $E_{j,s}^{\mathrm{in}}$ represents the interconnecting input vector (w.r.t. local controller s) for subnetwork s from neighboring subnetwork $j, E_{s,j}^{\mathrm{out}}$ represents the interconnecting output vector (w.r.t. local controller j) from neighboring subnetwork j to subnetwork s, and $E_{s,j}^{\mathrm{out}}(k) = K_{s,j}[x_j^T(k), y_j^T(k), u_j^T(k)]^T$, with $K_{s,j}$ the interconnecting output selection matrix from j to s.

Remark 2. Note that for freeway networks, the state vector x_s represents traffic state variables (i.e. speed, density, and flow), the output vector y_s represents quantities that can be computed by means of traffic state variables. The control input vector u_s corresponds to variable speed limits and ramp metering rates. The external uncontrollable input vector D_s^{in} corresponds to demands for origins and on-ramps. The interconnecting input vector E_s^{in} and the interconnecting output vector $E_{s,j}^{\mathrm{out}}$ correspond to upstream flows, upstream speeds, and downstream densities. The general constraint function F_s corresponds to constraints on speed variables, density variables, flow variables, variable speed limits, and ramp metering rates. The interconnecting constraints represented by (11) correspond to upstream flows, upstream speeds, and downstream densities among neighboring subnetworks.

In state space methods, state variables are usually independent from each other, and output variables can be computed by means of functions depending on the state variables. The centralized model predictive control problem can be formulated as follows:

$$\mathrm{Problem1}: \quad \min_{\widetilde{u}(k)} \sum_{s=1}^{N_{\mathrm{sub}}} J_s(\widetilde{x}_s(k), \widetilde{y}_s(k), \widetilde{u}_s(k)) \tag{5}$$

[2] The state vector x_s and output vector y_s are involved in the first term of (4), and the control input vector u_s is involved in all the three terms of (4).

$$\text{s.t.} \quad x_s(k+z+1) = f_s\left(x_s(k+z), u_s(k+z), D_s^{\text{in}}(k+z), E_s^{\text{in}}(k+z)\right) \quad \text{for } z = 0, \ldots, N_p - 1 \tag{6}$$

$$y_s(k+z) = h_s(x_s(k+z)) \quad \text{for } z = 1, \ldots, N_p \tag{7}$$

$$x_s(k) = x_s^k \tag{8}$$

$$u_s(k+z) = u_s(k+N_c-1) \quad \text{for } z = N_c, \ldots, N_p - 1 \tag{9}$$

$$F_s(\widetilde{x}_s(k), \widetilde{y}_s(k), \widetilde{u}_s(k)) \leqslant 0 \tag{10}$$

$$E_{j,s}^{\text{in}}(k+z) - E_{s,j}^{\text{out}}(k+z) = 0 \ \text{ for } j \in S_s, \ z = 0, \ldots, N_p - 1 \tag{11}$$

where u is a stacked variable containing the control input vectors for all subnetworks, $\sum_{s=1}^{N_{\text{sub}}} J_s\left(\widetilde{x}_s(k), \widetilde{y}_s(k), \widetilde{u}_s(k)\right)$ represents the overall control objective function, F_s is a general constraint function[3] on the states, outputs, and control inputs for subnetwork s over the prediction period, (11) represents the interconnecting constraints among subnetwork s and all neighbors. In addition, the variables $\widetilde{x}_s(k), \widetilde{y}_s(k), \widetilde{u}_s(k)$ and $\widetilde{u}(k)$ are defined as follows:

$$\widetilde{x}_s(k) = \left[x_s^T(k+1), \ldots, x_s^T(k+N_p)\right]^T \tag{12}$$

$$\widetilde{y}_s(k) = \left[y_s^T(k+1), \ldots, y_s^T(k+N_p)\right]^T \tag{13}$$

$$\widetilde{u}_s(k) = \left[u_s^T(k), \ldots, u_s^T(k+N_c-1)\right]^T \tag{14}$$

$$\widetilde{u}(k) = \left[u^T(k), \ldots, u^T(k+N_c-1)\right]^T \tag{15}$$

As an example, Fig. 1 shows the uncontrollable inputs and the interconnecting inputs and outputs for a network including 3 subnetworks in series. For a subnetwork, both the uncontrollable inputs and the interconnecting inputs can affect the dynamics of that subnetwork. The interconnecting outputs of a subnetwork can affect the dynamics of the neighbors of that subnetwork. Note that in this paper we only consider interconnecting *equality* constraints among individual subnetworks. However, it is possible to include other types of interconnecting constraints, such as interconnecting *inequality* constraints among individual subnetworks (e.g. an upper bound on the flow from an on-ramp to an adjacent stretch that belongs to another subnetwork).

According to (Negenborn et al., 2008; Bertsekas, 1982), the interconnecting constraints (i.e. (11)) can be merged into the overall control objective function in (5) by defining an augmented Lagrangian function as follows:

$$L\left(\widetilde{x}(k), \widetilde{y}(k), \widetilde{u}(k), \widetilde{\Lambda}^{\text{in}}(k)\right) = \sum_{s=1}^{N_{\text{sub}}} \left(J_s(\widetilde{x}_s(k), \widetilde{y}_s(k), \widetilde{u}_s(k)) + \sum_{j \in S_s} \left(\left(\widetilde{\lambda}_{j,s}^{\text{in}}(k)\right)^T \left(\widetilde{E}_{j,s}^{\text{in}}(k) - \widetilde{E}_{s,j}^{\text{out}}(k)\right) + \frac{c}{2} \left\| \widetilde{E}_{j,s}^{\text{in}}(k) - \widetilde{E}_{s,j}^{\text{out}}(k) \right\|_2^2 \right) \right) \tag{16}$$

where c is a positive constant, $\lambda_{j,s}^{\text{in}}$ represents the Lagrange multiplier vector corresponding to $E_{j,s}^{\text{in}}$, x and y are stacked variables respectively containing states and outputs for all subnetworks, $\Lambda^{\text{in}}(k)$ is a stacked vector containing all values of $\lambda_{j,s}^{\text{in}}$ for all subnetworks, and $\widetilde{x}(k), \widetilde{y}(k), \widetilde{\Lambda}^{\text{in}}(k), \widetilde{\lambda}_{j,s}^{\text{in}}(k), \widetilde{E}_{j,s}^{\text{in}}(k)$, and $\widetilde{E}_{s,j}^{\text{out}}(k)$ are defined in a similar way to $\widetilde{x}_s(k)$ (i.e. (12)) over the prediction period covering steps $k+z, z = 0, \ldots, N_p - 1$. For solving optimization problems, augmented Lagrangian functions and Lagrange multipliers are often used for dealing with constraints, i.e. for transforming constrained optimization problems into unconstrained optimization problems. For more details readers can refer to (Negenborn et al., 2008; Bertsekas, 1982).

According to duality theory (Negenborn et al., 2008; Bertsekas, 1982; Boyd and Vandenberghe, 2004), the dual problem associated with the original problem (Problem 1 defined by (5)–(11)) is defined as maximizing (16) over the Lagrange multipliers while minimizing (16) over the control inputs, i.e. as follows:

$$\text{Problem2}: \quad \max_{\widetilde{\Lambda}^{\text{in}}(k)} \ \min_{\widetilde{u}(k)} L\left(\widetilde{x}(k), \widetilde{y}(k), \widetilde{u}(k), \widetilde{\Lambda}^{\text{in}}(k)\right) \tag{17}$$

$$\text{s.t. } (6) - (10) \quad \text{for } s = 1, \ldots, N_{\text{sub}}$$

[3] Note that (10) comprises all equality and inequality constraints on the states, outputs, and control inputs, such as inequality constraints for limiting the maximum queue lengths at on-ramps.

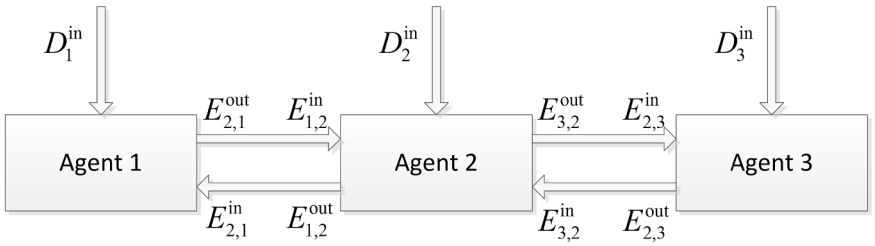

Fig. 1. Uncontrollable inputs and interconnecting inputs and outputs for an example network.

Referring to (Negenborn et al., 2008; Camponogara et al., 2002; Bertsekas, 1982), it can be proved that if the local control objective functions (i.e. J_s in (5)) and the inequality constraints (i.e. (10)) of subnetworks are convex and the equality constraints (i.e. (11)) of subnetworks are affine, the solution of the original problem (Problem 1) can be obtained by iteratively solving the dual problem (Problem 2). As described in (Negenborn et al., 2008; Camponogara et al., 2002; Bertsekas, 1982), in the procedure for solving the dual problem (Problem 2), for each iteration the Lagrange multipliers are estimated using the solution for the previous iteration, and next they are kept fixed for that iteration. Note that when Lagrange multipliers are fixed, only the minimization problem is solved for the dual problem (Problem 2). An iteration here means that the minimization in Problem 2 is solved once for a given set of fixed Lagrange multipliers at time step k. The minimization in the dual problem (Problem 2) should be iteratively solved until the Lagrange multipliers do not change anymore up to a predefined tolerance. In this case it has been proved that the solution of the dual problem (Problem 2) is equivalent to the solution of the original problem (Problem 1) in (Bertsekas, 1982). For more details, readers can refer to (Negenborn et al., 2008; Camponogara et al., 2002; Bertsekas, 1982).

In order to solve the centralized control problem by means of DMPC, the augmented Lagrangian function (16), which is not separable due to the quadratic terms, needs to be distributed to local controllers. In the literature, some approaches have been developed for decomposing couplings similar to the quadratic terms, such as block coordinate descent (Negenborn et al., 2008), dual ascent (Boyd et al., 2011), auxiliary problem principle (Kim and Baldick, May 1997). Moreover, in Section 5 we have introduced a specific Eq. (39) for $J_{s,g}^{\text{inter}}$ for the ADMM approach (Boyd et al., 2011). In the following text, J_s^{inter} is the function handling the interconnecting variables determined by local controller s, $E_{j,s}^{\text{out}}$ represents the interconnecting output vector (w.r.t. local controller s) from subnetwork s to neighboring subnetwork j, $\lambda_{j,s}^{\text{out}}$ represents the Lagrange multiplier vector corresponding to $E_{j,s}^{\text{out}}$, and $\widetilde{\lambda}_{j,s}^{\text{out}}(k)$ is defined in a similar way to $\widetilde{x}_s(k)$ (i.e. (12)) over the prediction period covering steps $k+z, z=0,\ldots,N_{\text{p}}-1$. With the above mentioned approaches, the centralized control problem can be distributed to local controllers, and a local controller iteratively solves the following problem with fixed Lagrange multipliers within one iteration:

$$\text{Problem3}: \quad \min_{\substack{\sim \\ u_s(k),\, \widetilde{E}_s^{\text{in}}(k),\, \widetilde{E}_s^{\text{out}}(k)}} \left(J_s(\widetilde{x}_s(k), \widetilde{y}_s(k), \widetilde{u}_s(k)) + \sum_{j \in S_s} J_s^{\text{inter}}\left(\widetilde{\lambda}_{j,s}^{\text{in}}(k), \widetilde{\lambda}_{j,s}^{\text{out}}(k), \widetilde{E}_{j,s}^{\text{in}}(k), \widetilde{E}_{j,s}^{\text{out}}(k)\right) \right) \tag{18}$$

$$\text{s.t. } (6)-(10) \quad \text{for } s = 1, \ldots, N_{\text{sub}}.$$

Remark 3. The prediction model METANET considered in this paper is nonlinear and nonconvex, and therefore the resulting optimization problem for MPC is nonlinear and nonconvex. In this paper, we apply DMPC for nonlinear-nonconvex traffic networks, and investigate the control effectiveness by a numerical experiment.

4. Scenario-Based Distributed Model Predictive Control

4.1. Uncertainties in Large-Scale Freeway Networks

4.1.1. Global Uncertainties and Local Uncertainties

In freeway networks, uncertainties can be introduced through various sources, such as the measurements of traffic states, the external uncontrollable inputs, the parameters of prediction models, and so on. For example, uncertainties are usually introduced in the process of measuring traffic states due to factors like the accuracy of sensors. Similarly, uncertainties are often introduced in the procedure of estimating the external uncontrollable inputs, such as demands and boundary conditions. Furthermore, uncertainties are also introduced in the procedure of calibrating the parameters of the prediction models. More specifically, the accuracy of the parameters of the prediction models for freeway networks can be affected by various uncertain factors, such as weather conditions (e.g. sunny or rainy), traffic compositions (e.g. cars and trucks), and extra flows to some destinations caused by events (e.g. a pop concert or a soccer game). Particularly, the weather conditions can affect free-flow speeds; the traffic compositions can affect the accuracy of most model parameters; extra flows to some destinations can affect turning rates at intersections.

The uncertainties for freeway networks can be described in different ways. For instance, uncertainties often fall within some confidence bands around the nominal profiles; thus uncertainties can be described by means of some bounded sets including all the

possible values of the uncertainties. Uncertainties can also be described by building a library of the possible scenarios for the uncertainties, and the possibilities of the appearances for these scenarios can be estimated. Note that bounded sets can be used for describing an infinite number of realizations of uncertainties, while a library of scenarios can be used for describing a finite number of uncertainty scenarios. In this paper, we assume that the uncertainties are described by means of a library consisting of finite sets that cover all possible scenarios of uncertainties. In this case, it is possible to use an expected-value setting (which is probabilistic) for robust control, based on the probabilities for uncertainty scenarios.

In order to develop a scenario-based DMPC approach that can handle uncertainties for large-scale freeway networks, we divide the uncertainties in the considered overall network into two categories, i.e. global uncertainties and local uncertainties. The global uncertainties are those uncertainties that apply to the overall network, e.g. the uncertainties in network-wide global weather conditions. The local uncertainties are those uncertainties that apply to a single subnetwork, including the uncertainties in local weather conditions, local traffic compositions, local demands at origins, boundary conditions, the measurements of traffic states, and so on. We define a set for global scenarios and a set for local uncertainties. In particular, Ω_{glo} is defined as the set of all the possible global scenarios, and $\Omega_{\text{loc},s}$ is defined as the set of all the possible local scenarios for subnetwork s. The global scenarios in Ω_{glo} apply to all subnetworks, while the local scenarios in $\Omega_{\text{loc},s}$ only apply to subnetwork s.

Distinguishing global scenarios from local scenarios can reduce the size of the scenario tree w.r.t. the case that all uncertainties are considered in the same way. The number of combinations of the local scenarios for all subnetworks is $\prod_{s=1,\ldots,N_{\text{sub}}} N_{\text{loc},s}$, with $N_{\text{loc},s}$ the number of the local scenarios for subnetwork s. If global uncertainties are considered in the same way as local uncertainties, there will be N_{glo} scenarios for each subnetwork corresponding to global uncertainties, and the number of possible combinations is $N_{\text{glo}}^{N_{\text{sub}}}$. Otherwise, if global uncertainties are considered to be the same for all subnetworks, there will be N_{glo} combinations for global uncertainties for all subnetworks. The total number of combinations for all uncertainty scenarios is equal to the number of combinations for local scenarios multiplied by the number of combinations for global scenarios. Therefore, when global uncertainties are treated in a different way from local uncertainties, the number of combinations for all uncertainty scenarios is significantly reduced in comparison with the case that they are not distinguished.

4.1.2. Reduced Scenario Tree of Global and Local Uncertainties

A local controller in a distributed control scheme needs interconnecting inputs from neighboring subnetworks. For a given global scenario for a subnetwork, the interconnecting inputs from neighboring subnetworks are considered to be predicted for the same given global scenario. However, local uncertainties only apply to certain subnetworks; thus, for a given subnetwork s, any local scenario in $\Omega_{\text{L},j}$ may occur for neighboring subnetwork j.

When all the combinations of the local scenarios for all subnetworks are considered, i.e. a complete local scenario tree for local uncertainties is constructed, the total number of these combinations for a given global scenario is

$$N_{\text{com}} = \prod_{s=1,\ldots,N_{\text{sub}}} N_{\text{loc},s} \tag{19}$$

Thus the number of the combinations to be handled by a local controller is N_{com} for a given global scenario. In this case, the computational burden is large due to the large size of the complete local scenario tree.

In order to reduce the computational burden w.r.t. the complete local scenario tree, we propose a reduced local scenario tree, in which the interconnecting inputs for a subnetwork from neighboring subnetworks are assumed to be independent of the local scenarios for the neighboring subnetworks. The interconnecting inputs for a given subnetwork and the interconnecting outputs from the neighboring subnetworks to the given subnetwork describe the same physical quantities. Thus, the interconnecting outputs of a neighboring subnetwork are combined for all the local scenarios for that neighboring subnetwork, resulting in the combined interconnecting outputs corresponding to the interconnecting inputs for the given subnetwork.

We define the *reduced scenario tree* by combining all global scenarios and the reduced local scenario tree for the entire network. Similarly, we define the *complete scenario tree* by combining all global scenarios and the complete local scenario tree for the entire network. For subnetwork s, the number of combinations of global scenarios and local scenarios for the reduced scenario tree (i.e. $N_{\text{glo}}N_{\text{loc},s}$) is smaller than that for the complete scenario tree (i.e. $N_{\text{glo}}N_{\text{com}}$). Therefore, the computational burden for processing the

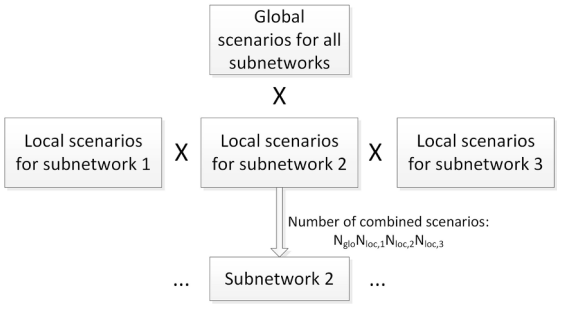

Fig. 2. Complete scenario tree for an example subnetwork with 2 neighbours (" × " means multiplication).

reduced scenario is relatively small w.r.t. that for processing the complete scenario tree. For clarification, Figs. 2 and 3 show the combination schemes for the complete scenario tree and the reduced scenario tree for a subnetwork (subnetwork 2) with 2 neighbours (subnetwork 1 and subnetwork 3). In the reduced scenario tree, local uncertainty scenarios are combined as 1 uncertainty scenario for a neighbouring subnetwork, as shown in Fig. 3. However, all local scenarios for that neighboring subnetwork are still included for the considered subnetwork, in the way of 1 combined scenario.

4.2. Scenario-Based DMPC with Global and Local Uncertainties

In this section, we develop a scenario-based DMPC approach based on the reduced scenario tree proposed in Section 4.1. For handling uncertainties in the scenario-based DMPC problem, we consider an expected-value setting (which is probabilistic) and a min–max setting.

In the following text, the symbols $J_{s,g}^{\text{inter}}, E_{s,g}^{\text{in}}, E_{s,g}^{\text{out}}, E_{j,s,g}^{\text{in}}, E_{s,j,g}^{\text{out}}, E_{j,s,g}^{\text{out}}, \Lambda_g^{\text{in}}, \lambda_{j,s,g}^{\text{in}}(k)$, and $\lambda_{j,s,g}^{\text{out}}$ have similar meanings to the corresponding symbols without subscript g in Section 3, but now they apply to the case with global uncertainties and combined local uncertainties; the symbols $x_{s,g,l}, y_{s,g,l}, J_{s,g,l}, f_{s,g,l}, F_{s,g,l}, D_{s,g,l}^{\text{in}}$, and $E_{j,s,g,l}^{\text{out}}$ have similar meanings to the corresponding symbols without subscripts g and l in Section 3, but now they are for the case with global uncertainties and local uncertainties. In addition, $\widetilde{x}_{s,g,l}(k)$, and $\widetilde{y}_{s,g,l}(k)$ are defined in a similar way to $\widetilde{x}_s(k)$ (i.e. (12)) over the prediction period covering steps $k+z, z=1,\ldots,N_{\text{p}}$; $\widetilde{E}_{j,s,g}^{\text{in}}(k), \widetilde{E}_{s,j,g}^{\text{out}}(k), \widetilde{E}_{j,s,g}^{\text{out}}(k), \widetilde{\Lambda}_g^{\text{in}}(k), \widetilde{\lambda}_{j,s,g}^{\text{in}}(k)$, $\widetilde{\lambda}_{j,s,g}^{\text{out}}(k)$, and $\widetilde{E}_{j,s,g,l}^{\text{out}}(k)$ are defined similarly to $\widetilde{x}_s(k)$ (i.e. (12)) over the prediction period covering steps $k+z, z=0,\ldots,N_{\text{p}}-1$.

In the following text, g is the index for the scenarios for global uncertainties, p_g is the probability of global scenario g, and ω_g represents scenario g for global uncertainties. Similarly, l is the index for the local scenarios for a subnetwork, $\omega_{s,l}$ represents scenario l for the local uncertainties for subnetwork s, $p_{s,l}$ is the probability of local scenario l for subnetwork s, and $p_{s,l}$ is assumed to be known in this paper.

4.2.1. Scenario-Based DMPC on the Basis of a Reduced Scenario Tree and an Expected-Value Setting

We have developed scenario-based DMPC by assuming that the probability for a specified scenario is known. Readers can refer to (Florescu, 2015; Ghahramani, 2018) for more details about how to obtain the probability for a specified scenario at different uncertainty levels. The centralized scenario-based MPC problem for the large-scale freeway network considered in Section 3 can be formulated as follows:

$$\text{Problem4}: \quad \min_{\widetilde{u}(k)} \sum_{g=1}^{N_{\text{glo}}} p_g \sum_{s=1}^{N_{\text{sub}}} \sum_{l=1}^{N_{\text{loc},s}} p_{s,l} J_{s,g,l}\left(\widetilde{x}_{s,g,l}(k), \widetilde{y}_{s,g,l}(k), \widetilde{u}_s(k)\right) \tag{20}$$

$$\text{s.t.} \quad \begin{aligned} & x_{s,g,l}\left(k+z+1\right) = f_{s,g,l}\left(x_{s,g,l}\left(k+z\right), u_s\left(k+z\right), D_{s,g,l}^{\text{in}}\left(k+z\right), \right. \\ & \left. E_{s,g}^{\text{in}}\left(k+z\right), \omega_g\left(k+z\right), \omega_{s,l}\left(k+z\right)\right) \quad \text{for } z=0,\ldots,N_{\text{p}}-1 \end{aligned} \tag{21}$$

$$y_{s,g,l}\left(k+z\right) = h_s\left(x_{s,g,l}\left(k+z\right)\right) \quad \text{for } z=1,\ldots,N_{\text{p}} \tag{22}$$

$$x_{s,g,l}\left(k\right) = x_s^k \tag{23}$$

$$\omega_g\left(k+z\right) \in \Omega_{\text{glo}}\left(k+z\right) \quad \text{for } z=0,\ldots,N_{\text{p}}-1 \tag{24}$$

$$\omega_{s,l}\left(k+z\right) \in \Omega_{\text{loc},s}\left(k+z\right) \quad \text{for } z=0,\ldots,N_{\text{p}}-1 \tag{25}$$

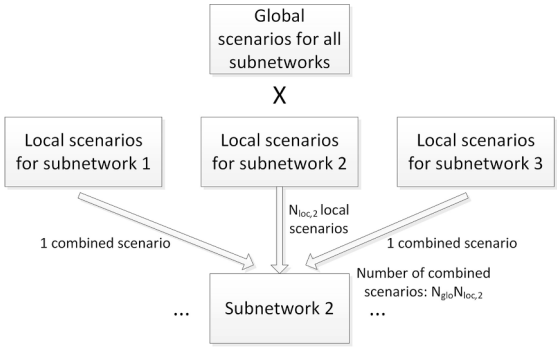

Fig. 3. Reduced scenario tree for an example subnetwork with 2 neighbours (" × " means multiplication).

$$F_{s,g,l}\left(\widetilde{x}_{s,g,l}(k),\widetilde{y}_{s,g,l}(k),\widetilde{u}_s(k)\right)\leqslant 0 \tag{26}$$

$$E^{\text{in}}_{j,s,g}\left(k+z\right)-E^{\text{out}}_{s,j,g}\left(k+z\right)=0 \quad \text{for } j\in S_s,\ z=0,\ldots,N_{\text{p}}-1 \tag{27}$$

Equation (9)

where $\sum_{g=1}^{N_{\text{glo}}}p_g\sum_{s=1}^{N_{\text{sub}}}\sum_{l=1}^{N_{\text{loc},s}}p_{s,l}J_{s,g,l}\left(\widetilde{x}_{s,g,l}(k),\widetilde{y}_{s,g,l}(k),\widetilde{u}_s(k)\right)$ represents the overall control objective function for scenario-based DMPC with global and local uncertainties. Eqs. (21) and (22) describe how the states and outputs of subnetwork s are determined with global and local uncertainties considered. Based on the reduced scenario tree, local scenarios are combined within a subnetwork for $E^{\text{in}}_{s,g}$, $E^{\text{in}}_{j,s,g}$, and $E^{\text{out}}_{s,j,g}$; thus there is no index l in these variables.

Referring to Eq. (16) and (Negenborn et al., 2008; Bertsekas, 1982), the augmented Lagrangian function with global and local uncertainties considered can be defined as follows:

$$L_{g,l}\left(\widetilde{x}_{\text{GL}}\left(k\right),\widetilde{y}_{\text{GL}}\left(k\right),\widetilde{u}\left(k\right),\widetilde{\Lambda}^{\text{in}}_{g}\left(k\right)\right)=\sum_{g=1}^{N_{\text{glo}}}p_g\sum_{s=1}^{N_{\text{sub}}}\sum_{l=1}^{N_{\text{loc},s}}p_{s,l}\left(J_{s,g,l}\left(\widetilde{x}_{s,g,l}(k),\widetilde{y}_{s,g,l}(k),\widetilde{u}_s(k)\right)+\sum_{j\in S_s}\left(\left(\widetilde{\lambda}^{\text{in}}_{j,s,g}\left(k\right)\right)^{T}\left(\widetilde{E}^{\text{in}}_{j,s,g}\left(k\right)-\widetilde{E}^{\text{out}}_{s,j,g}\left(k\right)\right)\right.\right.$$
$$\left.\left.+\frac{c}{2}\left\|\widetilde{E}^{\text{in}}_{j,s,g}\left(k\right)-\widetilde{E}^{\text{out}}_{s,j,g}\left(k\right)\right\|_2^2\right)\right) \tag{28}$$

where $\widetilde{x}_{\text{GL}}(k)$ is a stacked variable containing the states of all subnetworks for all global scenarios and local scenarios over all steps in the prediction period from k to $k+N_{\text{p}}-1$, and where $\widetilde{y}_{\text{GL}}(k)$ is a stacked variable containing the outputs of all subnetworks for all global scenarios and local scenarios over all steps in the prediction period from k to $k+N_{\text{p}}-1$.

Note that Eq. (28) is analogous to Eq. (16). Similar to the case without uncertainties considered in Section 3, each subnetwork is assigned a local controller, which determines the optimal local control inputs. For handling uncertainties in the joint constraint on the states, outputs, and control inputs, (26) can be incorporated into the local control objective functions via penalty terms. As described in Section 3, the quadratic terms in (28) can be decomposed for different subnetworks. In the following text, γ is a relatively high weight w.r.t. the weights for $J_{s,g,l}$ and $J^{\text{inter}}_{s,g}$. Moreover, the order of magnitude of γ should be higher than those of the weights for $J_{s,g,l}$ and $J^{\text{inter}}_{s,g}$. Similar to Section 3, we let each local controller iteratively solve the following scenario-based control problem:

$$\text{Problem5}: \quad \min_{\widetilde{u}_s(k),\ \widetilde{E}^{\text{in}}_{s,g}(k),\ \widetilde{E}^{\text{out}}_{s,g}(k)}\ \sum_{g=1}^{N_{\text{glo}}}p_g\sum_{l=1}^{N_{\text{loc},s}}p_{s,l}\left(J_{s,g,l}\left(\widetilde{x}_{s,g,l}(k),\widetilde{y}_{s,g,l}(k),\widetilde{u}_s(k)\right)+\gamma\max\left(F_{s,g,l}\left(\widetilde{x}_{s,g,l}(k),\widetilde{y}_{s,g,l}(k),\widetilde{u}_s(k)\right),0\right)\right.$$
$$\left.+\sum_{j\in S_s}J^{\text{inter}}_{s,g}\left(\widetilde{\lambda}^{\text{in}}_{j,s,g}\left(k\right),\widetilde{\lambda}^{\text{out}}_{j,s,g}\left(k\right),\widetilde{E}^{\text{in}}_{j,s,g}\left(k\right),\widetilde{E}^{\text{out}}_{j,s,g}\left(k\right)\right)\right) \tag{29}$$

s.t. (9), (21) – (25)

where $J_{s,g,l}$ is defined according to Eq. (4). Similarly to Section 3, the Lagrange multipliers are fixed within one iteration of solving the scenario-based control problem for each subnetwork, and they are computed based on the solutions of the previous iteration. In the proposed scenario-based DMPC approach, information for predicting traffic behaviors is partial for local controllers. However, interconnections among neighboring controllers are included in local objective functions.

Corresponding to local controller s, the interconnecting outputs from subnetwork s to neighbouring subnetwork j are combined as follows in the expected-value setting:

$$\widetilde{E}^{\text{out}}_{j,s,g}\left(k\right)=\sum_{l=1}^{N_{\text{loc},s}}p_{s,l}\widetilde{E}^{\text{out}}_{j,s,g,l}\left(k\right) \tag{30}$$

This means that for two neighboring subnetworks, the information exchange between them is the same for all local scenarios for a given global scenario. For instance, for a network including 3 subnetworks in series, Fig. 4 shows the uncontrollable inputs and the interconnecting inputs and outputs for the case that includes both global scenarios and local scenarios. The uncontrollable inputs correspond to local scenarios, and the interconnecting inputs and outputs are combined for all local scenarios for global scenario g.

Remark 4. Note that for scenario-based DMPC on the basis of a reduced scenario tree, we can consider to keep the P-percentile of the most likely scenarios in Ω_{glo} and $\Omega_{\text{loc},s}$, with the rest unlikely scenarios thrown away. This is helpful for finding a trade-off between performance and computation time.

4.2.2. Scenario-Based DMPC on the Basis of a Reduced Scenario Tree and a Min–Max Setting

In the min–max setting, the centralized scenario-based MPC problem for the large-scale freeway network considered in Section 3 can be formulated as follows:

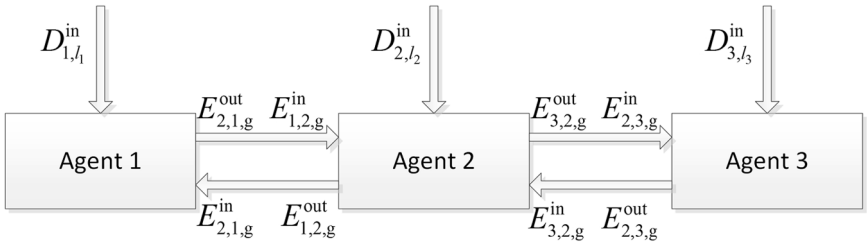

Fig. 4. Information exchange for an example network with both global uncertainties and local uncertainties.

$$\text{Problem6}: \quad \min_{\widetilde{u}(k)} \max_{g=1,\ldots,N_{\text{glo}}} \sum_{s=1}^{N_{\text{sub}}} \max_{l=1,\ldots,N_{\text{loc},s}} J_{s,g,l}\left(\widetilde{x}_{s,g,l}(k), \widetilde{y}_{s,g,l}(k), \widetilde{u}_s(k)\right) \tag{31}$$

$$\text{s.t. } (9), (21)-(27)$$

Referring to Eqs. (16) and (28), and (Negenborn et al., 2008; Bertsekas, 1982), for the min–max setting the augmented Lagrangian function with global and local uncertainties considered can be defined as follows:

$$L_{g,l}\left(\widetilde{x}_{\text{GL}}(k), \widetilde{y}_{\text{GL}}(k), \widetilde{u}(k), \widetilde{\Lambda}^{\text{in}}_g(k)\right) = \max_{g=1,\ldots,N_{\text{glo}}} \sum_{s=1}^{N_{\text{sub}}} \max_{l=1,\ldots,N_{\text{loc},s}} \left(J_{s,g,l}\left(\widetilde{x}_{s,g,l}(k), \widetilde{y}_{s,g,l}(k), \widetilde{u}_s(k)\right) + \sum_{j\in S_s}\left(\left(\widetilde{\lambda}^{\text{in}}_{j,s,g}(k)\right)^T\left(\widetilde{E}^{\text{in}}_{j,s,g}(k) - \widetilde{E}^{\text{out}}_{s,j,g}(k)\right)\right.\right.$$
$$\left.\left. + \frac{c}{2}\left\|\widetilde{E}^{\text{in}}_{j,s,g}(k) - \widetilde{E}^{\text{out}}_{s,j,g}(k)\right\|_2^2\right)\right) \tag{32}$$

Note that Eq. (32) is analogous to Eqs. (28) and (16). Similar to the Section 4.2.1, we let each local controller iteratively solve the following scenario-based control problem for scenario-based DMPC on the basis of the reduced scenario tree and the min–max setting:

$$\text{Problem7}: \quad \min_{\widetilde{u}_s(k),\, \widetilde{E}^{\text{in}}_{s,g}(k),\, \widetilde{E}^{\text{out}}_{s,g}(k)} \max_{g=1,\ldots,N_{\text{glo}}} \max_{l=1,\ldots,N_{\text{loc},s}} \left(J_{s,g,l}\left(\widetilde{x}_{s,g,l}(k), \widetilde{y}_{s,g,l}(k), \widetilde{u}_s(k)\right) + \gamma \max\left(F_{s,g,l}\left(\widetilde{x}_{s,g,l}(k), \widetilde{y}_{s,g,l}(k), \widetilde{u}_s(k)\right), 0\right)\right.$$
$$\left. + \sum_{j\in S_s} J^{\text{inter}}_{s,g}\left(\widetilde{\lambda}^{\text{in}}_{j,s,g}(k), \widetilde{\lambda}^{\text{out}}_{j,s,g}(k), \widetilde{E}^{\text{in}}_{j,s,g}(k), \widetilde{E}^{\text{out}}_{j,s,g}(k)\right)\right) \tag{33}$$

$$\text{s.t. } (9), (21)-(25)$$

where $J_{s,g,l}$ is defined according to Eq. (4). Eq. (33) is analogous to Eq. (29). In the same way as in Sections 3 and 4.2.1, the Lagrange multipliers are fixed within one iteration of solving the scenario-based control problem for each subnetwork, and they are computed based on the solutions of the previous iteration.

Corresponding to local controller s, the interconnecting outputs from subnetwork s to neighbouring subnetwork j are combined as follows in the min–max setting:

$$\widetilde{E}^{\text{out}}_{j,s,g}(k) = \max_{l=1,\ldots,N_{\text{loc},s}} \left\|\widetilde{E}^{\text{out}}_{j,s,g,l}(k) - \widetilde{E}^{\text{in}}_{s,j,g}(k)\right\|_2^2 \tag{34}$$

which corresponds to the local scenario for subnetwork s that leads to the maximum distance between $\widetilde{E}^{\text{out}}_{j,s,g,l}(k)$ and $\widetilde{E}^{\text{in}}_{s,j,g}(k)$. Note that other alternatives[4] for defining $\widetilde{E}^{\text{out}}_{j,s,g}$ can also be considered.

5. Alternating Direction Method of Multipliers (ADMM) for Scenario-Based DMPC

In this section, we mainly apply ADMM to the new scenario-based DMPC approach developed in Section 4.2. More specifically, we adopt the "General Form Consensus Optimization" stated in Chapter 7.2 of (Boyd et al., 2011), where the dual decomposition method and the augmented Lagrangian method are used for decomposing the overall optimization problem into local optimization problems.

[4] An alternative way to define $\widetilde{E}^{\text{out}}_{j,s,g}(k)$ in the min–max setting can e.g. be

$$\widetilde{E}^{\text{out}}_{j,s,g}(k) = \max_{l=1,\ldots,N_{\text{loc},s}} J^{\text{inter}}_{s,g}\left(\widetilde{\lambda}^{\text{in}}_{j,s,g}(k), \widetilde{\lambda}^{\text{out}}_{j,s,g}(k), \widetilde{E}^{\text{in}}_{j,s,g}(k), \widetilde{E}^{\text{out}}_{j,s,g,l}(k)\right)$$

In Chapter 7.2 of (Boyd et al., 2011), global variables are used for describing couplings among subnetworks. The interconnecting inputs of subnetwork s from subnetwork j should ideally equal the interconnecting outputs of subnetwork j to subnetwork s, since they correspond to the same quantities. These interconnecting inputs and outputs for different subnetworks corresponding to the same quantities should converge to the same global variables by negotiation iterations among local controllers. For a specific combination of global scenario and local scenario, the number (N_{gv}) of global variables is

$$N_{\mathrm{gv}} = \sum_{s=1}^{N_{\mathrm{sub}}} N_s^{\mathrm{nb}} \tag{35}$$

where N_s^{nb} represents the number of the neighbors of subnetwork s.

Based on the setting in Section 4.2, the overall global variable for global scenario g is defined as $G_g(k) = [(G_{g,1}(k))^T, \ldots, (G_{g,N_{\mathrm{gv}}}(k))^T]^T$. The quantity $G_{j,s,g}$ is the global variable corresponding to the interconnecting variable from subnetwork j to subnetwork s for global scenario g. Both $\widetilde{G}_g(k)$ and $\widetilde{G}_{j,s,g}(k)$ are defined in a similar way to $\widetilde{x}_s(k)$ (i.e. (12)) over the prediction period covering steps $k+z, z = 0, \ldots, N_{\mathrm{p}}-1$. In the following text, $P_{j,s}$ is the matrix for selecting the global variable corresponding to the interconnecting variable from subnetwork j to subnetwork s. Thus the following relationship holds:

$$\widetilde{G}_{j,s,g}(k) = P_{j,s}\widetilde{G}_g(k) \tag{36}$$

In order to apply ADMM, the interconnecting constraint (27) should be replaced with

$$\begin{cases} \widetilde{E}^{\mathrm{in}}_{j,s,g}(k) - \widetilde{G}_{j,s,g}(k) = 0 \\ \widetilde{E}^{\mathrm{out}}_{s,j,g}(k) - \widetilde{G}_{j,s,g}(k) = 0 \end{cases} \text{for } j \in S_s \tag{37}$$

Note that if (34) is used for defining $\widetilde{E}^{\mathrm{out}}_{j,s,g}(k), \widetilde{E}^{\mathrm{in}}_{s,j,g}(k)$ should be replaced by $\widetilde{G}_{s,j,g}(k)$, since interconnecting variables should converge to global variables in ADMM:

$$\widetilde{E}^{\mathrm{out}}_{j,s,g}(k) = \max_{l=1,\ldots,N_{\mathrm{loc},s}} \left\| \widetilde{E}^{\mathrm{out}}_{j,s,g,l}(k) - \widetilde{G}_{s,j,g}(k) \right\|_2^2 \tag{38}$$

In the following text, σ represents the negotiation iteration number. The function $J^{\mathrm{inter}}_{s,g}$ is defined as follows:

$$\begin{aligned} &J^{\mathrm{inter}}_{s,g}\left(\left(\widetilde{\lambda}^{\mathrm{in}}_{j,s,g}(k)\right)_\sigma, \left(\widetilde{\lambda}^{\mathrm{out}}_{j,s,g}(k)\right)_\sigma, \left(\widetilde{E}^{\mathrm{in}}_{j,s,g}(k)\right)_{\sigma+1}, \left(\widetilde{E}^{\mathrm{out}}_{j,s,g}(k)\right)_{\sigma+1}\right) \\ &= \begin{bmatrix} \left(\widetilde{\lambda}^{\mathrm{in}}_{j,s,g}(k)\right)_\sigma \\ \left(\widetilde{\lambda}^{\mathrm{out}}_{j,s,g}(k)\right)_\sigma \end{bmatrix}^T \begin{bmatrix} \left(\widetilde{E}^{\mathrm{in}}_{j,s,g}(k)\right)_{\sigma+1} \\ \left(\widetilde{E}^{\mathrm{out}}_{j,s,g}(k)\right)_{\sigma+1} \end{bmatrix} + \frac{c}{2} \left\| \begin{bmatrix} \left(\widetilde{E}^{\mathrm{in}}_{j,s,g}(k)\right)_{\sigma+1} - \left(\widetilde{G}_{j,s,g}(k)\right)_\sigma \\ \left(\widetilde{E}^{\mathrm{out}}_{j,s,g}(k)\right)_{\sigma+1} - \left(\widetilde{G}_{s,j,g}(k)\right)_\sigma \end{bmatrix} \right\|_2^2 \end{aligned} \tag{39}$$

where both $\lambda^{\mathrm{in}}_{j,s,g}$ and $\lambda^{\mathrm{out}}_{j,s,g}$ are determined by local controller s. Note that for a local controller s, Eq. (39) is incorporated into Problem 5 or Problem 7.

The algorithm for the scenario-based DMPC approach based on the reduced scenario tree is described as follows:

1. Initialization: let $\sigma = 1$ and $\epsilon_\sigma = \infty$, and set an appropriate value for c. For $s = 1, \ldots, N_{\mathrm{sub}}$, let $x_s(k)$ equal the measured state variable x_s^k; let $u_s(k)$ equal the initial control input variable; estimate $\widetilde{D}^{\mathrm{in}}_{s,g,l}(k)$ according to historical data; let $(\widetilde{\lambda}^{\mathrm{in}}_{j,s,g}(k))_\sigma = 0$ and $(\widetilde{\lambda}^{\mathrm{out}}_{j,s,g}(k))_\sigma = 0$; and initialize $(\widetilde{G}_{j,s,g}(k))_\sigma$ and $(\widetilde{G}_{s,j,g}(k))_\sigma$ by a warm start [5].
2. For $s = 1, \ldots, N_{\mathrm{sub}}$, in a parallel fashion or a serial fashion local controller s determines $(\widetilde{u}_s(k))_{\sigma+1}, (\widetilde{E}^{\mathrm{in}}_{j,s,g}(k))_{\sigma+1}$, and $(\widetilde{E}^{\mathrm{out}}_{j,s,g}(k))_{\sigma+1}$ for $j \in S_s$ by solving the local problem defined by Problem 5 or Problem 7 with Eq. (39) being incorporated.
3. For $s = 1, \ldots, N_{\mathrm{sub}}$, update the global variables for all pairs of s and $j \in S_s$:

$$(\widetilde{G}_{s,j,g}(k))_{\sigma+1} = \frac{1}{2}\left(\left(\widetilde{E}^{\mathrm{in}}_{s,j,g}(k)\right)_{\sigma+1} + \left(\widetilde{E}^{\mathrm{out}}_{j,s,g}(k)\right)_{\sigma+1} \right) \tag{40}$$

4. For $s = 1, \ldots, N_{\mathrm{sub}}$, update the Lagrange multipliers for all pairs of s and $j \in S_s$:

[5] In the warm start, we assume that for the first control step the control inputs equal the initial control inputs over the prediction period, and that for other control steps the control inputs over the prediction period are estimated by shifting one step ahead the optimal control input sequence obtained at the previous control step, based on the receding-horizon scheme (Maciejowski, 2002; Camacho and Bordons, 2007).

$$\left(\widetilde{\lambda}^{\text{in}}_{j,s,g}\left(k\right)\right)_{\sigma+1} = \left(\widetilde{\lambda}^{\text{in}}_{j,s,g}\left(k\right)\right)_{\sigma} + c\left(\left(\widetilde{E}^{\text{in}}_{j,s,g}\left(k\right)\right)_{\sigma+1} - \left(\widetilde{G}_{j,s,g}\left(k\right)\right)_{\sigma+1}\right) \tag{41}$$

$$\left(\widetilde{\lambda}^{\text{out}}_{j,s,g}\left(k\right)\right)_{\sigma+1} = \left(\widetilde{\lambda}^{\text{out}}_{j,s,g}\left(k\right)\right)_{\sigma} + c\left(\left(\widetilde{E}^{\text{out}}_{j,s,g}\left(k\right)\right)_{\sigma+1} - \left(\widetilde{G}_{s,j,g}\left(k\right)\right)_{\sigma+1}\right) \tag{42}$$

5. Check the stopping condition:

$$\epsilon_{\sigma+1} = \left\| \begin{bmatrix} \left(\left(\widetilde{\Lambda}^{\text{in}}_{1}\left(k\right)\right)_{\sigma+1} - \left(\widetilde{\Lambda}^{\text{in}}_{1}\left(k\right)\right)_{\sigma}\right)^{T} \\ \vdots \\ \left(\left(\widetilde{\Lambda}^{\text{in}}_{N_{\text{glo}}}\left(k\right)\right)_{\sigma+1} - \left(\widetilde{\Lambda}^{\text{in}}_{N_{\text{glo}}}\left(k\right)\right)_{\sigma}\right)^{T} \\ \left(\left(\widetilde{\Lambda}^{\text{out}}_{1}\left(k\right)\right)_{\sigma+1} - \left(\widetilde{\Lambda}^{\text{out}}_{1}\left(k\right)\right)_{\sigma}\right)^{T} \\ \vdots \\ \left(\left(\widetilde{\Lambda}^{\text{out}}_{N_{\text{glo}}}\left(k\right)\right)_{\sigma+1} - \left(\widetilde{\Lambda}^{\text{out}}_{N_{\text{glo}}}\left(k\right)\right)_{\sigma}\right)^{T} \end{bmatrix} \right\|_{\infty} \tag{43}$$

where $\Lambda^{\text{out}}_{g}(k)$ is a stacked vector containing all values of $\lambda^{\text{out}}_{j,s}$ for all subnetworks, corresponding to global uncertainty scenario g. If $\epsilon_{\sigma+1} < \epsilon$ (ϵ: a small positive value), stop the optimization, and output $(\widetilde{u}_s(k))_{\sigma+1}$. Otherwise, go to step 2.

Remark 5. According to Remark 3, we apply DMPC for nonlinear-nonconvex traffic networks, and investigate the control effectiveness by a numerical experiment in this paper. As mentioned in Step 2 above, local controller s determines $(\widetilde{u}_s(k))_{\sigma+1}, (\widetilde{E}^{\text{in}}_{j,s,g}(k))_{\sigma+1}$, and $(\widetilde{E}^{\text{out}}_{j,s,g}(k))_{\sigma+1}$ at iteration σ. If we assume that $(\widetilde{E}^{\text{in}}_{j,s,g}(k))_{\sigma+1} = (\widetilde{E}^{\text{out}}_{s,j,g}(k))_{\sigma}$, the function $J^{\text{inter}}_{s,g}$ can be written as follows:

$$J^{\text{inter}}_{s,g}\left(\left(\widetilde{\lambda}^{\text{out}}_{j,s,g}\left(k\right)\right)_{\sigma}, \left(\widetilde{E}^{\text{out}}_{j,s,g}\left(k\right)\right)_{\sigma+1}\right) = \left(\widetilde{\lambda}^{\text{out}}_{j,s,g}\left(k\right)\right)^{T}_{\sigma}\left(\widetilde{E}^{\text{out}}_{j,s,g}\left(k\right)\right)_{\sigma+1} + \frac{c}{2}\left\|\left(\widetilde{E}^{\text{out}}_{j,s,g}\left(k\right)\right)_{\sigma+1} - \left(\widetilde{G}_{s,j,g}\left(k\right)\right)_{\sigma}\right\|^{2}_{2} \tag{44}$$

In this case, a local controller optimizes its local objective function on the basis of interconnecting outputs determined by neighbouring local controllers at previous iteration. Note that in essence local controllers still seek to converge with their neighbors by iteratively solving local control problems.

6. Case Study

6.1. Benchmark Network

We consider a freeway network as shown in Fig. 5 for the case study. In this freeway network, there are 10 links ($m = 1,\ldots,10$), 1 mainstream origin (O_0), 1 unrestricted destination (D_0), 3 on-ramps (O_1, O_2, and O_3), and 3 unrestricted off-ramps (O_4, O_5, and O_6). In total, these 10 links are divided into 18 segments with equal length $L_m = 1$ km. The mainstream stretch includes 2 lanes, and each on-ramp or each off-ramp includes 1 single lane. The positions of variable speed limits ($N_{\text{VSL}} = 6$) are shown in Fig. 5, and all on-ramps are metered ($N_{\text{RM}} = 3$). The queue lengths at all on-ramps are limited within 100 veh for avoiding spill back to upstream stretches. This queue length constraint corresponds to Eq. (26), which represents a constraint on states, outputs and control inputs. The turning rates at all off-ramps are assumed to be fixed as 5% of the mainstream flow. For applying scenario-based DMPC, the network is divided into 3 subnetworks (S_1, S_2, and S_3), and each subnetwork includes 6 segments, 1 on-ramp, and 1 off-ramp.

For subnetwork S_1, the interconnecting input is the density of the first segment of subnetwork S_2; the interconnecting outputs include the flow and speed of the last segment of subnetwork S_1. For subnetwork S_2, the interconnecting inputs include the flow and speed of the last segment of subnetwork S_1, and the density of the first segment of subnetwork S_3; the interconnecting outputs include the flow and speed of the last segment of subnetwork S_2. For subnetwork S_3, the interconnecting inputs include the flow and speed of the last segment of subnetwork S_2; the interconnecting output is the density of the first segment of subnetwork S_3.

The traffic flow model METANET described in Section 2 is used as both the process model and the prediction model. In this paper, we mainly focus on investigating the efficiency of scenario-based DMPC for traffic networks, neglecting the model mismatch caused by the difference between the prediction model and real traffic process. In fact, other traffic models can also be used as prediction models

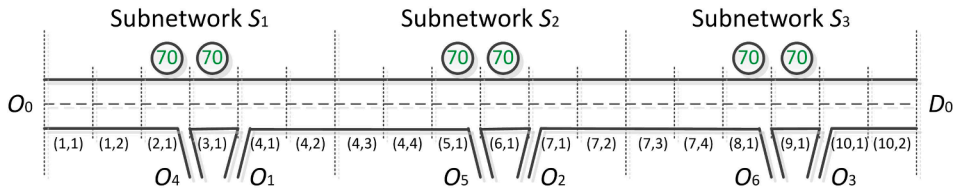

Fig. 5. The freeway network used for the case study.

Table 2
Parameters for case study.

C_{main}	2100 veh/h/lane	ξ_{TTS}	1
C_{onramp}	2000 veh/h/lane	ξ_{speed}	0.1
τ	18 s	ξ_{ramp}	0.1
$s\eta$	60 km^2/h	γ	100
κ	40 veh/km/lane	T	10 s
a_m	1.867	T_c	180 s
δ_m	0.1	N_p	3
v_m^{free}	102 km/h	N_c	2
ρ_m^{crit}	33.5 veh/km/lane		
$\rho_m^{\max}$	180 veh/km/lane		

in this approach. To some extent, the model mismatch issue can be addressed by state-of-the-art feedback control approaches such as MPC (Camacho and Bordons, 2007), by means of an inherent feedback scheme. The nominal parameters for METANET are chosen according to (Kotsialos et al., 2002; Hegyi et al., 2005). As suggested in (Hegyi et al., 2005), the prediction horizon is chosen according to the average time needed for a vehicle to go through the considered subnetwork. Table 2 includes the nominal parameters for METANET, time step parameters[6], prediction horizon, control horizon, and the weights in Problem 5 and Problem 7.

The considered simulation period is 2.5 h, and Fig. 6 shows the nominal demands for the mainstream origin and on-ramps.

6.2. Control Settings

6.2.1. Uncertainty Scenarios

In this section, we describe the global and local uncertainty scenarios used for the case study. In following text, we introduce the global and local uncertainty scenarios for simulations. In this section, we introduce the global and local uncertainty scenarios for Scenario-Based DMPC.

- *Uncertainty Scenarios for the Simulations*

  Uncertainties in weather conditions (sunny or rainy) are considered as *global uncertainties* for the overall network. We suppose that the model parameter τ and the free-flow speed v_m^{free} are affected by weather conditions. For sunny days, τ and v_m^{free} are considered to be nominal values given in Section 6.1. For rainy days, τ is considered to be 5% larger than the corresponding nominal value, i.e. $\tau = 18.9$ s, and v_m^{free} is considered to be 5% smaller than the corresponding nominal value, i.e. $v_m^{\text{free}} = 96.9$ km/h. The probability for sunny days is assumed to be 0.8, and the probability for rainy days is assumed to be 0.2.

  Uncertainties in demands are considered as *local uncertainties* for subnetworks. Based on nominal demands, three base demand scenarios over the entire simulation period are considered for constructing scenarios for simulations and scenario-based DMPC:
  - Base demand scenario 1: nominal demands with a probability of 0.7;
  - Base demand scenario 2: 90% of nominal demands with a probability of 0.1;
  - Base demand scenario 3: 110% of nominal demands with a probability of 0.2.

  In this case study, we consider 10 pre-selected demand scenarios for the simulations, of which the sampling step length is assumed to be equal to the control time step interval. Each of these 10 demand scenarios is pre-selected as follows: for each origin and at every sampling step the demand is randomly set to be one of the 3 base demand scenarios with the corresponding probabilities (i.e., 0.7, 0.1, 0.2). In the considered 10 demand scenarios for the simulations, 8 are for sunny days, and the remaining 2 are for rainy days. Note that in this case study, the demand scenarios are *local uncertainty scenarios*, while the weather scenarios are *global uncertainty* scenarios. The scenarios for simulations are combinations of the considered demand scenarios and the weather scenarios. For sunny days, the traffic is congested in the whole network roughly during simulation time 0.3–2.3 h.

[6] In the case study, the general case with $T_c \neq T$ is considered, where T_c represents the control time step interval. Accordingly, k_c is the control time step counter, and $M = T_c/T$ is an integer. Thus in (3), $\sum_{z=k_cM}^{(k_c+N_p)M-1}$ is used instead of $\sum_{z=k}^{k+N_p-1}$. In (4), $\sum_{z=k_c}^{k_c+N_c-1}$ is used instead of $\sum_{z=k}^{k+N_c-1}$.

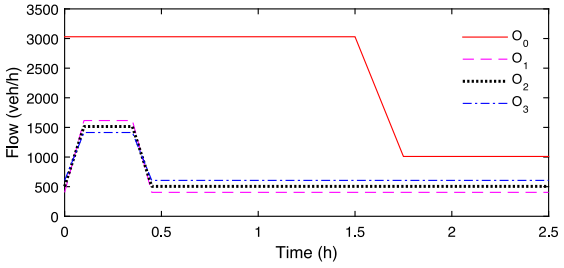

Fig. 6. Nominal demands for the mainstream origin and on-ramps.

For rainy days, the traffic is congested for segments 1–12 roughly during simulation time 0.3–2.3 h, and for segments 13–16 roughly during simulation time 0.3–2.5 h. During the congestion period, the minimum speed is about 10 km/h, corresponding to a strong congestion mode. For different uncertainty scenarios in demands, traffic conditions are roughly the same, while for rainy days the traffic is more congested than for sunny days.

- *Uncertainty Scenarios for Scenario-Based DMPC*

  For scenario-based DMPC, *global uncertainty scenarios* include sunny days and rainy days; demand scenarios (i.e. *local scenarios*) are constructed based on the base demand scenarios. If all the possible combinations of the 3 base demand scenarios are considered, then for a given origin and for a given control step, there are 27 (i.e. $(3\ \text{base scenarios})^{N_p}$) possible demand scenarios over the prediction period. The probability of each of these 27 demand scenarios is obtained by multiplying the probabilities of the selected base demand scenarios for all sampling steps over the prediction period. Next, we ignore the demand scenarios with probabilities lower than 0.02, which leaves 10 demand scenarios over the prediction period for each origin at every control step, of which the total probability is 0.868. Thus the number of the considered demand scenarios for each origin at each control step is significantly reduced, while the total probability is still large. Note that in the expected-value setting the probability for each of the remaining 10 demand scenarios needs to be divided by 0.868, so that the equivalent total probability equals 1. The same 10 demand scenarios are also considered in the min–max setting.

6.2.2. Control Approaches

Since our aim is to develop an approach to deal with the large-scale network control problem with uncertainties being directly handled, the following control approaches are considered:

- Nominal DMPC: based on nominal parameters and nominal demands, i.e. general DMPC without considering the scenario-based scheme for dealing with uncertainties when optimizing the control inputs;
- Scenario-Based DMPC 1: based on the reduced scenario tree and the expected-value setting, i.e. Problem 5;
- Scenario-Based DMPC 2: based on the reduced scenario tree and the min–max setting, i.e. Problem 7.

For Scenario-Based DMPC 2, (38) is used for determining interconnecting outputs for global scenarios, and the Eq. (44) in Remark 5 is used for computing $J_{s,g}^{\text{inter}}$.

6.2.3. Other Control Settings

All approaches are implemented in a serial scheme, i.e. local controllers solve local optimization problems in a serial fashion, taking into account the latest information of neighboring local controllers (Negenborn et al., 2008). For all approaches, we set a fixed computation time for every control time step. This fixed computation time includes all computations including negotiation iterations among controllers in series for every control step (note that in this case the stopping condition (43) is not used). We consider four cases in this paper, i.e. the maximum allowed computation time for every control step for all control approaches is respectively set to be 3 min, 10 min, 15 min, and 20 min for each case.[7] In practice, the computation time for each control step is required to be less than T_c, and this can e.g. be realized by means of fast implementation or parallel implementation, which are outside the scope of this paper.

In the simulations, all optimization problems are solved by the "TOMLAB" optimization tool, with the prediction model METANET coded in C. All simulations are implemented on a computer with 12 Intel(R) Core(TM) i7-8750H CPU @2.20 GHz processors.

6.3. Results and Analysis

6.3.1. Performance

In Tables 3–5, for a control approach, the average and standard deviation of the results for all simulation scenarios are listed. In

[7] Note that in this paper we make the maximum allowed computation time for different approaches equal for fair comparison.

Table 3
Simulation results for nominal DMPC.

Fixed Computation Time		$T_c = 3$ min	$T_c = 10$ min	$T_c = 15$ min	$T_c = 20$ min
J_{TTS}^{imp}	Average	6.93%	6.93%	6.99%	6.96%
	Standard deviation	0.81%	0.78%	0.75%	0.79%
J_{pen}	Average	12.92%	13.39%	13.47%	13.53%
	Standard deviation	4.59%	4.82%	4.84%	4.81%
J_{tot}^{imp}	Average	-7.04%	-7.56%	-7.59%	-7.69%
	Standard deviation	4.593%	5.19%	5.23%	5.21%

Table 4
Simulation results for scenario-based DMPC 1.

Fixed Computation Time		$T_c = 3$ min	$T_c = 10$ min	$T_c = 15$ min	$T_c = 20$ min
J_{TTS}^{imp}	Average	5.59%	6.38%	6.47%	6.53%
	Standard deviation	0.75%	0.70%	0.76%	0.86%
J_{pen}	Average	0%	0%	0%	0%
	Standard deviation	0%	0%	0%	0%
J_{tot}^{imp}	Average	5.59%	6.38%	6.47%	6.53%
	Standard deviation	0.75%	0.70%	0.76%	0.86%

Table 5
Simulation results for scenario-based DMPC 2.

Fixed Computation Time		$T_c = 3$ min	$T_c = 10$ min	$T_c = 15$ min	$T_c = 20$ min
J_{TTS}^{imp}	Average	4.62%	5.58%	5.92%	5.95%
	Standard deviation	0.55%	0.61%	0.74%	0.68%
J_{pen}	Average	0%	0%	0%	0%
	Standard deviation	0%	0%	0%	0%
J_{tot}^{imp}	Average	4.62%	5.58%	5.92%	5.95%
	Standard deviation	0.55%	0.61%	0.74%	0.68%

these tables, J_{TTS}^{imp} represents the relative improvement in TTS w.r.t. the no-control case over the entire simulation period, J_{pen} represents the maximum of the relative queue constraint violations[8] for all on-ramps over the entire simulation period, J_{tot}^{imp} represents the relative improvement in the total performance[9] w.r.t. the no-control case, and the total performance is defined as $J_{tot} = \frac{TTS_{total}}{TTS_{nom}} + \gamma J_{pen}$, with TTS_{total} the total time spent over the entire simulation period in a closed-loop simulation.

From Tables 3–5 we can see that for nominal DMPC the total performance is worse than that for the no-control case, while for scenario-based DMPC the total performance is improved w.r.t. the case without control. More specifically, the TTS can be improved by nominal DMPC, but the queue constraints are not satisfied, leading to a worse total performance than the no-control case. For scenario-based DMPC, the TTS is improved less than nominal DMPC, but the queue constraints are satisfied, resulting in an improvement of the total performance. This means that scenario-based DMPC is more robust than nominal DMPC for this case study.

With the increase of the computation time for each control step, the total performance is further improved by scenario-based DMPC approaches; however, this not the case for nominal DMPC. This is probably due to the fact that nominal DMPC does not take into

[8] The relative queue constraint violation for an on-ramp o is defined as $\max\left(\max_{k=1,\ldots,k_{end}} \frac{w_o(k)}{w_o^{max}} - 1, 0\right)$, where k_{end} represents the last simulation time step of the entire simulation period, and w_o^{max} represents the maximum permitted queue length for on-ramp o.

[9] The J_{tot}^{imp} reported in this section is corresponding to objective functions defined in Problem 5 and Problem 7, where $J_{s,g}^{inter}$ and penalty terms on variable speed limits and ramp metering rates defined in Eq. (4) are ignorable w.r.t. the queue length constraint term (i.e. the term with γ included in Problem 5 and Problem 7. Thus we compared J_{tot}^{imp} in this section.

account uncertainties by means of the scenario-based scheme: Although there is an inherent feedback scheme in nominal DMPC, the corresponding control inputs obtained in a longer fixed computation time for each control step may result in a worse total performance, due to constraint violations, as shown in Tables 3–5.

Moreover, the standard deviations of $J_{\mathrm{TTS}}^{\mathrm{imp}}$,$J_{\mathrm{pen}}$, and $J_{\mathrm{tot}}^{\mathrm{imp}}$ are all small for scenario-based DMPC. However, the standard deviations of J_{pen} and $J_{\mathrm{tot}}^{\mathrm{imp}}$ are relatively large for nominal DMPC. This shows that scenario-based DMPC results in a more consistent total performance than nominal DMPC.

Comparing scenario-based DMPC for the expected-value setting (Scenario-Based DMPC 1) with scenario-based DMPC for the min–max setting (Scenario-Based DMPC 2), we can see that for this case study using the expected-value setting can improve the total performance more than using the min–max setting. This is probably due to the fact that the same uncertainty scenarios are used for the expected-value setting and the min–max setting. For the min–max setting the worst case of the total performance among all the considered uncertainty scenarios is optimized, resulting in more conservative control inputs than those for the expected-value setting.

6.3.2. *Traffic behaviours and control inputs*

In this section, one simulation scenario is chosen as an example, for which the variable speed limits and the ramp metering rates for all the considered approaches are plotted in Figs. 7 and 8. The corresponding origin flows, queue lengths, speeds, and densities for that simulation scenario are shown in Figs. 9–12, describing traffic behaviours for the no-control case and all the considered control schemes.

From Fig. 7 we can see that the variable speed limits determined by scenario-based DMPC are more fluctuating than those determined by nominal DMPC. From Fig. 8 we can see that the ramp metering rates determined by scenario-based DMPC slightly fluctuate in comparison with those determined by nominal DMPC. The fluctuations in the control inputs determined by scenario-based DMPC are probably due to the fact that it takes into account multiple uncertainty scenarios by means of the scenario-based scheme, while nominal DMPC takes into account only one nominal scenario. Besides, since we have a nonlinear-nonconvex problem, at every control step the solutions of the local controllers in general converge to local optima instead of a global optimum of the centralized control problem; this could also lead to fluctuations in the control inputs. From our point of view, these fluctuations are acceptable when the control time step length equals 3 min.

From Fig. 9, we can see that there is a capacity drop around time $t = 0.75$ h for the no-control case. For nominal DMPC, scenario-based DMPC 1, and scenario-based DMPC2, this capacity drop disappears. This means that the considered control schemes in this paper can reduce traffic congestion for the given settings. From Fig. 10, we can see that for nominal DMPC, the queue length constraint at on-ramp O_2 is violated. This means that nominal DMPC cannot ensure the satisfaction of queue length constraints. Fig. 11 shows speed profiles for the no control case and all the considered approaches, and Fig. 12 shows density profiles for the no control case and all the considered approaches. We can see that the density profiles for scenario-based DMPC are similar to those for nominal DMPC. However, there are slight fluctuations in speed profiles for scenario-based DMPC, corresponding to those fluctuations in variable speed limits.

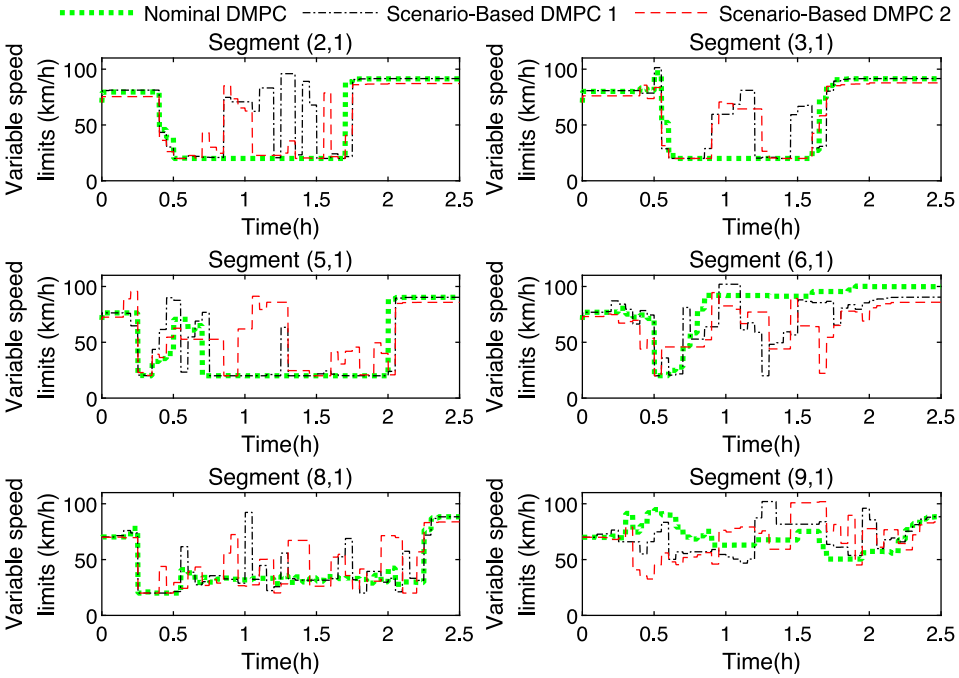

Fig. 7. Variable speed limits for all the considered approaches.

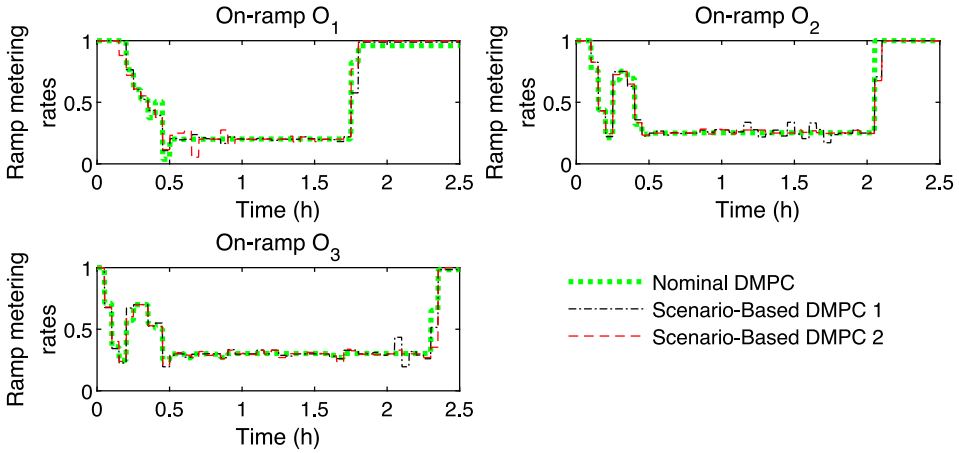

Fig. 8. Ramp metering rates for all the considered approaches.

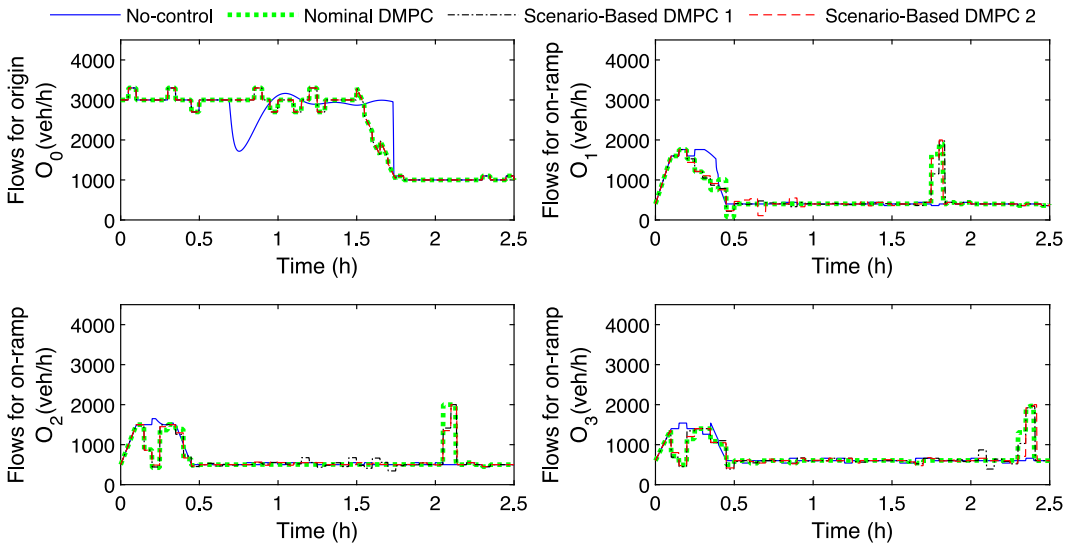

Fig. 9. Origin flows for all the considered approaches.

6.3.3. Computational Efficiency w.r.t. the Complete Scenario Tree

In the case study, we did not apply scenario-based DMPC on the basis of the complete scenario tree. For evaluating the computational efficiency of the complete scenario tree, we select the scenario-based DMPC approach based on the complete scenario tree and the expected-value setting as a reference case for testing. The scheme for this reference case is described in Appendix A. In this section, we implement simulations based on the parameters in Table 2. As an example, the simulations are implemented for one of the uncertainty scenarios for simulations(as described in Section 6.2).

We first make a rough estimate of the computation time $t_{\star}$ needed for solving the local optimization problems for all 3 controllers in a serial way, i.e. for 1 negotiation iteration. Then, we estimate the number N_{ite} of iterations needed for a single run of simulation for the entire simulation period. In this section, we consider that scenario-based DMPC on the basis of the complete scenario tree needs the same number of negotiation iterations as scenario-based DMPC on the basis of the reduced scenario tree. Then, the rough computation time $t_{\triangle}$ needed for scenario-based DMPC on the basis of the complete scenario tree for the entire simulation period (2.5 h) is obtained by multiplying $t_{\star}$ with N_{ite}.

We estimate $t_{\star}$ by averaging the time needed for one negotiation iteration at the first control step, the middle control step, and the last control step. According to the test, it takes roughly 14 h for finishing one negotiation iteration for scenario-based DMPC on the basis of the complete scenario tree, i.e. $t_{\star} = 14$ h. For the case that the computation time for every control step is fixed as 3 min, the

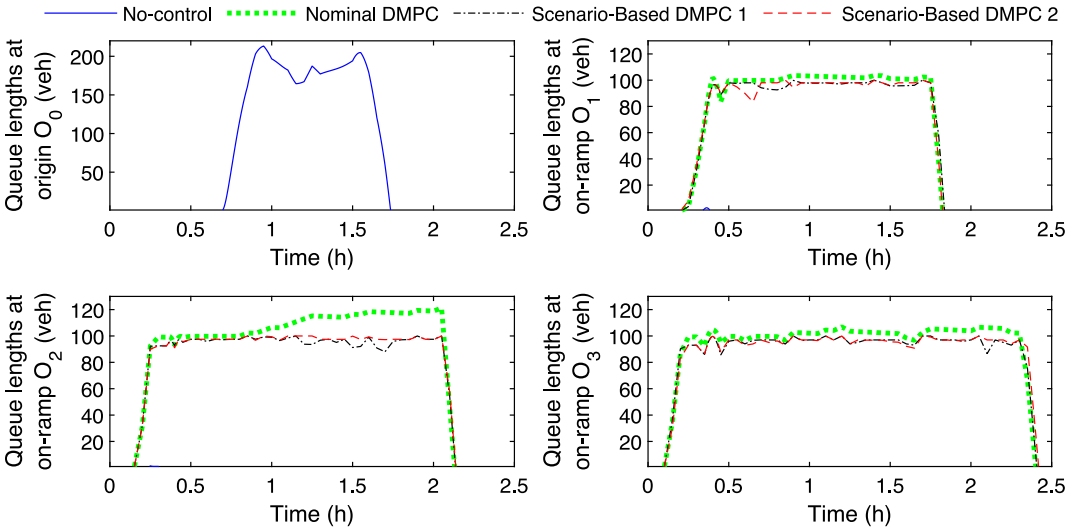

Fig. 10. Queue lengths for all the considered approaches.

total number of negotiation iterations for a single run for scenario-based DMPC on the basis of the reduced scenario tree is about $N_{\text{ite}} = 500$. Hence, it would take about $t_{\triangle} = 7000$ h for finishing 500 negotiation iterations. This is much longer than the computation time for scenario-based DMPC on the basis of the reduced scenario tree, which is 2.5 h (i.e. the entire simulation time length) for the case that the fixed computation time for a control step is 3 min (i.e. the control time step length).

According to the above discussion we can conclude that the computational efficiency of scenario-based DMPC on the basis of the reduced scenario tree is much higher than that of scenario-based DMPC on the basis of the complete scenario tree. Note that the main aim is to comparing the computational efficiency of the reduced tree method w.r.t. the complete scenario tree method. For applying the proposed scenario-based approaches in real time, fast implementation and parallel implementation can be used in the future.

Remark 6. For the centralized scheme there will be more variables to be optimized by a single controller (i.e. the centralized controller), while the complete scenario tree will still be used for taking into account the uncertainties. In fact, improving computational efficiency is the main motivation of using the DMPC approach, and our aim of this manuscript is to compare the cases with and without considering uncertainties. In addition, according to the simulation results of this paper, we can see that the scenario-based DPMC approaches that we proposed can indeed reduce traffic congestion, making the capacity drop in the no control case disappear. Therefore, we do not compare our control schemes with the centralized scheme in this paper.

7. Conclusions and Future Work

In this paper, we have developed a new scenario-based DMPC approach for freeway networks by distinguishing global uncertainties for the overall network from local uncertainties for particular subnetworks only. Instead of constructing a complete scenario tree with all the combinations of the local scenarios for all subnetworks considered, we have proposed to construct a reduced scenario tree by combining the interconnecting outputs for a subnetwork for all the local scenarios for that subnetwork. To reduce the computational burden, in the new scenario-based DMPC approach, an expected-value setting (which is probabilistic) and a min–max setting are considered for combining local scenarios and for defining objective functions for subnetworks, which include both control performance indices and constraint violation penalties.

We have illustrated by a numerical experiment that for scenario-based DMPC on the basis of the reduced scenario tree the total performance can be improved compared to the no-control case, with the queue constraints satisfied; while for nominal DMPC, the total performance could not be improved w.r.t. to the no-control case, due to the violation of the queue constraints. The experiment also showed that both the expected-value setting and the min–max setting are effective in improving the total performance.

For future work, we will focus on investigating how the complexity of the scenario-based DMPC approach increases with the size of a traffic network. The trade-off between the selection of subnetwork size and performance (i.e. the sensitivity analysis on how the size of subnetwork influences the final results) will also be considered as one of our future research topics. We will also consider to include correlation among the uncertainty scenarios of different subnetworks. In addition, more traffic scenarios, other types of uncertainties, different control actions for different global scenarios will be considered for studying and improving the effectiveness of the new scenario-based DMPC approach. Furthermore, we will consider to focus on the model mismatch between the prediction model and the

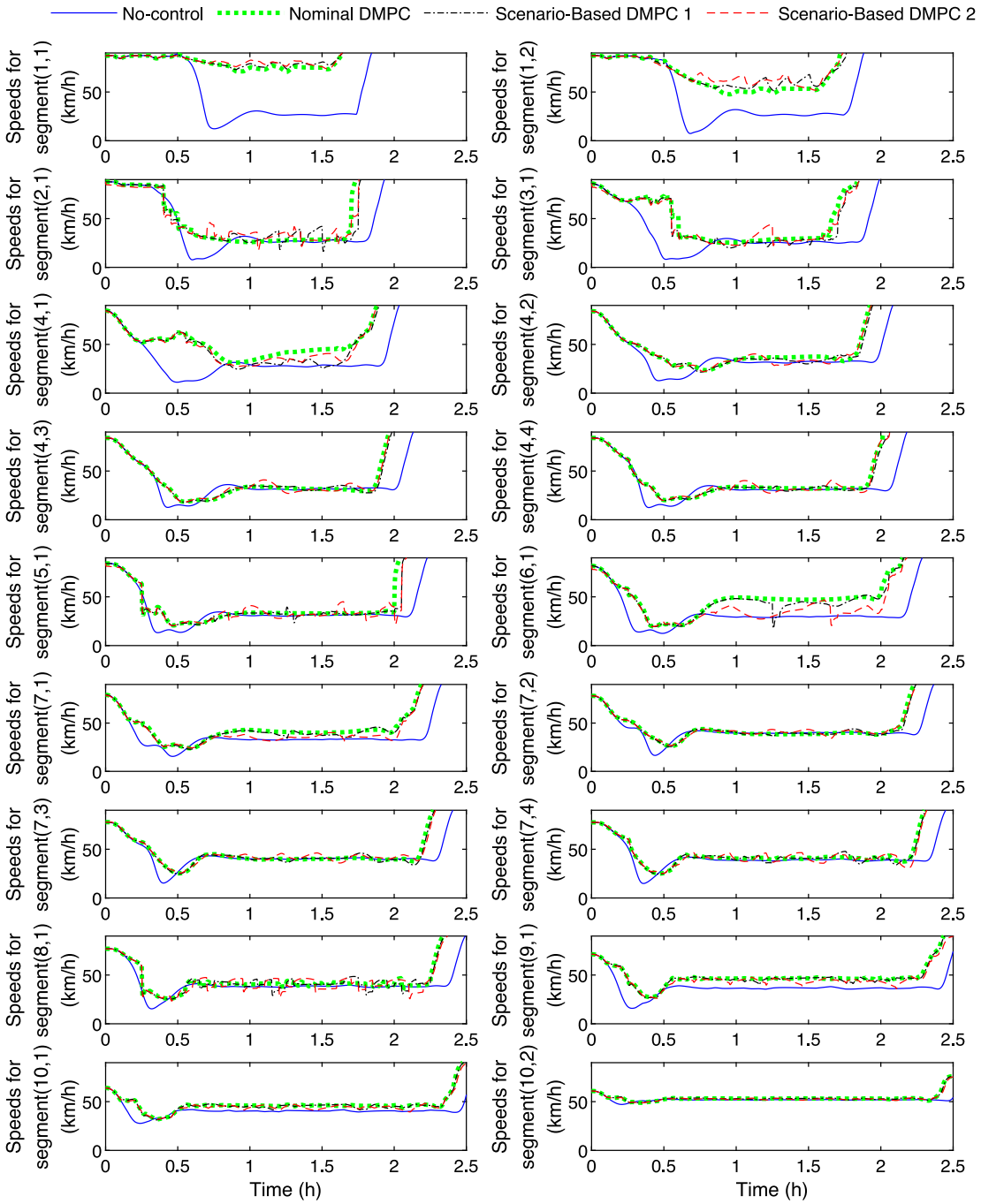

Fig. 11. Speeds for all the considered approaches.

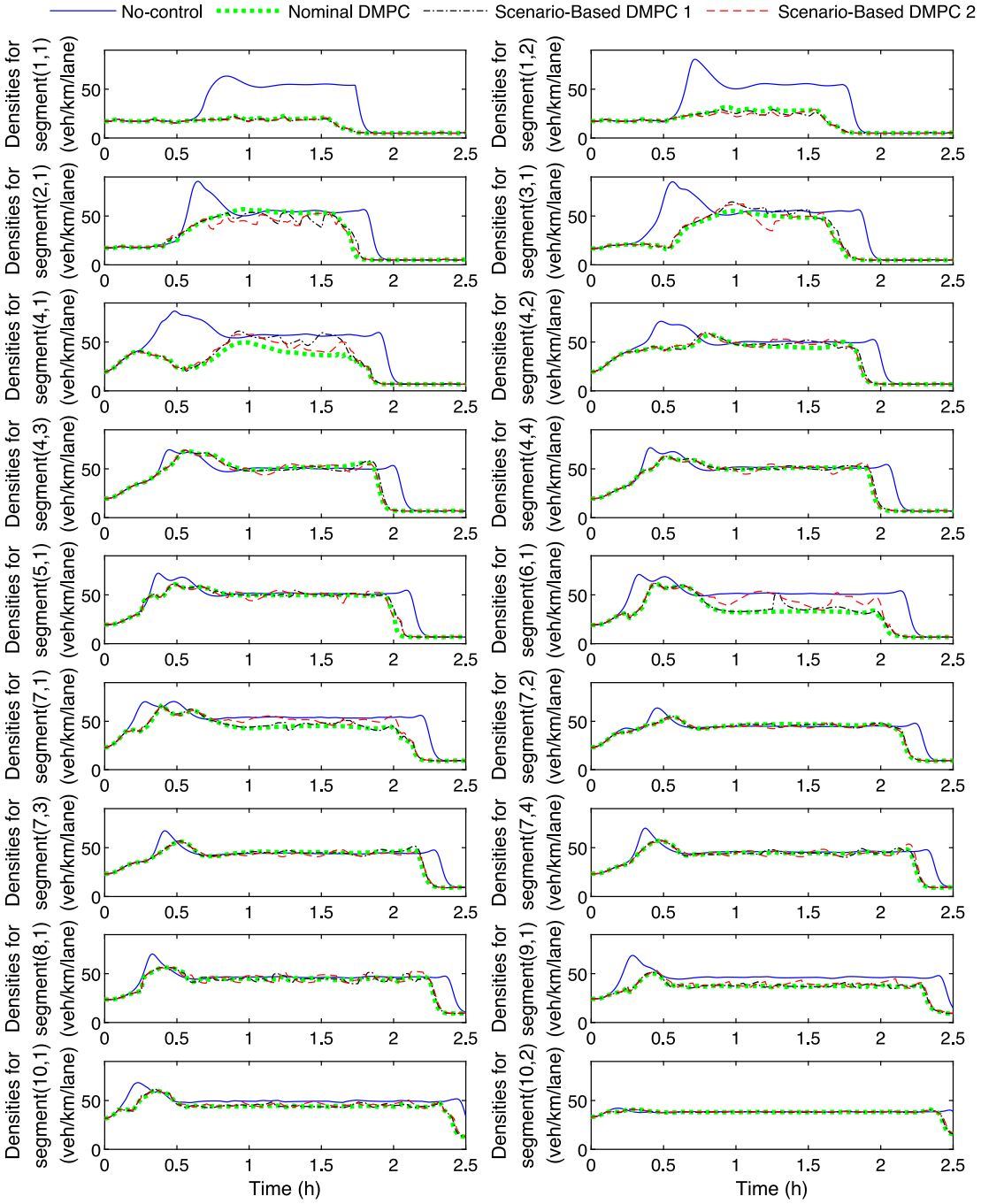

Fig. 12. Densities for all the considered approaches.

real traffic process, use of parallel computation, methods to divide a large traffic network into subnetworks, and further investigations on robustness, computability, and statistical properties, extensive analysis of suboptimality and convergence.

Appendix A. Scenario-Based DMPC on the Basis of the Complete Scenario Tree and the Expected-Value Setting

The aim of Appendix A is to include a comparison of the computational efficiency for scenario-based DMPC on the basis of the reduced scenario tree and the complete scenario tree. The formulas presented in Appendix A are analogous to Problem 5, except for the way of combing local uncertainty scenarios, as described in Section 4.1.

The scenario-based DMPC problem based on the complete scenario tree and the expected-value setting for a local agent s is defined as follows:

$$\min_{\widetilde{u}_s(k),\ \widetilde{E}^{\text{in}}_{s,g,\ell}(k),\ \widetilde{E}^{\text{out}}_{s,g,\ell}(k),} \sum_{g=1}^{N_{\text{glo}}} p_g \left(\sum_{\ell=1}^{N_{\text{com}}} p_\ell \left(J_{s,g,\ell}\left(\widetilde{x}_{s,g,\ell}(k), \widetilde{y}_{s,g,\ell}(k), \widetilde{u}_s(k)\right) \right. \right. \\ \left. + \gamma \left(\max\left(F_{s,g,\ell}\left(\widetilde{x}_{s,g,\ell}(k), \widetilde{y}_{s,g,\ell}(k), \widetilde{u}_s(k)\right), 0\right) \right. \right. \\ \left. \left. \left. + \sum_{j \in S_s} J^{\text{inter}}_{s,g,\ell}\left(\widetilde{\lambda}^{\text{in}}_{j,s,g,\ell}(k), \widetilde{\lambda}^{\text{out}}_{j,s,g,\ell}(k), \widetilde{E}^{\text{in}}_{j,s,g,\ell}(k), \widetilde{E}^{\text{out}}_{j,s,g,\ell}(k)\right) \right) \right) \right) \tag{45}$$

$$\text{s.t.} \quad \begin{aligned} & x_{s,g,\ell}(k+z+1) = f_{s,g,\ell}\left(x_{s,g,\ell}(k+z), u_s(k+z), D^{\text{in}}_{s,g,\ell}(k+z), \right. \\ & \left. E^{\text{in}}_{s,g,\ell}(k+z), \omega_g(k+z), \omega_\ell(k+z)\right) \quad \text{for } z = 0, \ldots, N_{\text{p}} - 1 \\ & y_{s,g,\ell}(k+z) = h_s\left(x_{s,g,\ell}(k+z)\right) \quad \text{for } z = 1, \ldots, N_{\text{p}} \end{aligned} \tag{46}$$

$$x_{s,g,\ell}(k) = x^k_s \tag{47}$$

$$\begin{aligned} & \omega_\ell(k+z) \in \Omega_{\text{L},1}(k+z) \times \ldots \times \Omega_{\text{L},N_{\text{sub}}}(k+z) \quad \text{for } z = 0, \ldots, N_{\text{p}} - 1 \\ & \text{Equations (9) and (24)} \\ & \text{for } g = 1, \ldots, N_{\text{glo}}, \text{ and } l = 1, \ldots, N_{\text{com}} \end{aligned}$$

where ω_ℓ represents a combined local uncertainty scenario for all subnetworks in the complete scenario tree, and p_ℓ is the probability for ω_ℓ. The symbols $x_{s,g,\ell}, y_{s,g,\ell}, J_{s,g,\ell}, F_{s,g,\ell}, J^{\text{inter}}_{s,g,\ell}, f_{s,g,\ell}, \lambda^{\text{in}}_{j,s,g,\ell}, \lambda^{\text{out}}_{j,s,g,\ell}, E^{\text{in}}_{j,s,g,\ell}, E^{\text{out}}_{j,s,g,\ell}, D^{\text{in}}_{s,g,\ell}, E^{\text{in}}_{s,g,\ell}$, and $E^{\text{out}}_{s,g,\ell}$ have similar meanings to corresponding symbols without subscripts g and ℓ in Section 3, but now they are for the case with global uncertainties and combined local uncertainty scenarios for all subnetworks. In addition, $\widetilde{x}_{s,g,\ell}(k)$ and $\widetilde{y}_{s,g,\ell}(k)$, are defined similarly to $\widetilde{x}_s(k)$ (i.e. (12)) over the prediction horizon covering steps $k+z, z = 1, \ldots, N_{\text{p}}$; $\widetilde{\lambda}^{\text{in}}_{j,s,g,\ell}(k), \widetilde{\lambda}^{\text{out}}_{j,s,g,\ell}(k), \widetilde{E}^{\text{in}}_{j,s,g,\ell}(k)$, and $\widetilde{E}^{\text{out}}_{j,s,g,\ell}(k)$ are defined in a similar way to $\widetilde{x}_s(k)$ (i.e. (12)) over the prediction horizon covering steps $k+z, z = 0, \ldots, N_{\text{p}} - 1$.

References

D. Bernardini and A. Bemporad. Scenario-based model predictive control of stochastic constrained linear systems. In Proceedings of the Joint 48th IEEE Conference on Decision and Control and 28th Chinese Control Conference, pages 6333–6338, Shanghai, China, December 2009.

Bertsekas, D.P., 1982. Constrained Optimization and Lagrange Multiplier Methods. Academic Press, London, United Kingdom.

Boyd, S., Vandenberghe, L., 2004. Convex Optimization. Cambridge University Press, Cambridge, United Kingdom.

Boyd, S., Parikh, N., Chu, E., Peleato, B., Eckstein, J., 2011. Distributed optimization and statistical learning via the alternating direction method of multipliers. Foundations and Trends in Machine Learning 3 (1), 1–122.

Calafiore, G.C., Campi, M.C., 2006. The scenario approach to robust control design. IEEE Trans. Autom. Control 51 (5), 742–753.

Calafiore, G.C., Fagiano, L., 2013. Robust model predictive control via scenario optimization. IEEE Trans. Autom. Control 58 (1), 219–224.

Camacho, E.F., Bordons, C., 2007. Model Predictive Control. Springer-Verlag, London, United Kingdom.

P.J. Campo and M. Morari. Robust model predictive control. In Proceedings of the American Control Conference, pages 1021–1026, Minneapolis, USA, June 1987.

Camponogara, E., Jia, D., Krogh, B.H., Talukdar, S., 2002. Distributed model predictive control. IEEE Control Syst. Mag. 22 (1), 44–52.

Christofides, P.D., Scattolini, R., de la Peña, D.M., Liu, J., 2013. Distributed model predictive control: A tutorial review and future research directions. Computers & Chemical Engineering 51, 21–41.

Daganzo, C.F., 1995. The cell transmission model, part II: Network traffic. Transportation Research Part B: Methodological 29 (2), 79–93.

De Nicolao, G., Magni, L., Scattolini, R., 1998. Stabilizing receding-horizon control of nonlinear time-varying systems. IEEE Trans. Autom. Control 43 (7), 1030–1036.

de Souza, F.A., Camponogara, E., Kraus Junior, W., Peccin, V.B., 2014. Distributed mpc for urban traffic networks: A simulation-based performance analysis. Optimal Control Applications and Methods 36 (3), 353–368.

A. Ferrara, A. Nai Oleari, S. Sacone, and S. Siri. Freeways as systems of systems: A distributed model predictive control scheme. IEEE Systems Journal, 9(1), 312–323, March 2015.

A. Ferrara, S. Sacone, and S. Siri. Event-triggered model predictive schemes for freeway traffic control. Transportation Research Part C: Emerging Technologies, 58 (Special Issue: Advanced Road Traffic Control):554–567, September 2015.

Florescu, I., 2015. Probability and Stochastic Processes. John Wiley & Sons Inc, New Jersey, USA.

Frejo, J.R.D., Camacho, E.F., 2012. Global versus local MPC algorithms in freeway traffic control with ramp metering and variable speed limits. IEEE Trans. Intell. Transp. Syst. 13 (4), 1556–1565.

Ghahramani, S., 2018. Fundamentals of Probability With Stochastic Processes. CRC Press, Florida, USA.

P. Giselsson. Output feedback distributed model predictive control with inherent robustness properties. In Proceedings of the American Control Conference, pages 1691–1696, Washington, DC, USA, June 2013.
Giselsson, P., Doan, M.D., Keviczky, T., De Schutter, B., Rantzer, A., 2013. Accelerated gradient methods and dual decomposition in distributed model predictive control. Automatica 49 (3), 829–833.
Gruber, J.K., Ramírez, D.R., Limon, D., Alamo, T., 2013. Computationally efficient nonlinear min-max model predictive control based on Volterra series models-Application to a pilot plant. J. Process Control 23 (4), 543–560.
Haddad, J., Mirkin, B., 2016. Adaptive perimeter traffic control of urban road networks based on mfd model with time delays. Int. J. Robust Nonlinear Control 26 (6), 1267–1285.
Han, Y., Hegyi, A., Yuan, Y., Hoogendoorn, S., Papageorgiou, M., 2017. Resolving freeway jam waves by discrete first-order model-based predictive control of variable speed limits. Transp. Res. Part C 77, 405–420.
Hegyi, A., De Schutter, B., Hellendoorn, J., 2005. Model predictive control for optimal coordination of ramp metering and variable speed limits. Transportation Research Part C: Emerging Technologies 13 (3), 185–209.
R. Hoyer and U. Jumar. Fuzzy control of traffic lights. In Proceedings of 1994 IEEE 3rd International Fuzzy Systems Conference, pages 1526–1531 vol 3, Orlando, FL, USA, June 1994.
Kato, N., Fadlullah, Z.M., Mao, B., Tang, F., Akashi, O., Inoue, T., Mizutani, K., 2017. The deep learning vision for heterogeneous network traffic control: Proposal, challenges, and future perspective. IEEE Wirel. Commun. 24 (3), 146–153.
Kim, B.H., Baldick, R., May 1997. Coarse-grained distributed optimal power flow. IEEE Trans. Power Syst. 12 (2), 932–939.
E.S. Kim, S. Sadraddini, C. Belta, M. Arcak, and S.A. Seshia. Dynamic contracts for distributed temporal logic control of traffic networks. In 2017 IEEE 56th Annual Conference on Decision and Control (CDC), pages 3640–3645, Melbourne, VIC, Australia, December 2017.
Kotsialos, A., Papageorgiou, M., Mangeas, M., Haj-Salem, H., 2002. Coordinated and integrated control of motorway networks via non-linear optimal control. Transportation Research Part C: Emerging Technologies 10 (1), 65–84.
Le, T., Vu, H.L., Nazarathy, Y., Vo, B., Hoogendoorn, S., 2013. Linear-quadratic model predictive control for urban traffic networks. Procedia-Social and Behavioral Sciences 80, 512–530.
C. Leidereiter, A. Potschka, and H.G. Bock. Dual decomposition for QPs in scenario tree NMPC. In Proceedings of the European Control Conference, pages 1608–1613, Linz, Austria, July 2015.
Li, H., Shi, Y., 2014. Robust distributed model predictive control of constrained continuous-time nonlinear systems: A robustness constraint approach. IEEE Trans. Autom. Control 59 (6), 1673–1678.
Liu, S., Sadowska, A., Frejo, J.R.D., Núñez, A., Camacho, E.F., Hellendoorn, H., De Schutter, B., 2016. Robust receding horizon parameterized control for multi-class freeway networks: A tractable scenario-based approach. Int. J. Robust Nonlinear Control 26 (6), 1211–1245.
Shuai Liu, A. Sadowska, H. Hellendoorn, and B. De Schutter. Scenario-based distributed model predictive control for freeway networks. In 2016 IEEE 19th International Conference on Intelligent Transportation Systems (ITSC), pages 1779–1784, Rio de Janeiro, Brazil, November 2016.
Liu, S., Hellendoorn, H., De Schutter, B., 2017. Model predictive control for freeway networks based on multi-class traffic flow and emission models. IEEE Trans. Intell. Transp. Syst. 18 (2), 306–320.
Luo, Lihua, Ge, Ying-En, Zhang, Fangwei, Ban, Xuegang, 2016. Real-time route diversion control in a model predictive control framework with multiple objectives: Traf?c ef?ciency, emission reduction and fuel economy. Transp. Res. Part D 48, 332–356.
Maciejowski, J.M., 2002. Predictive Control: with Constraints. Person Education, London, United Kingdom.
Maestre, J.M., Negenborn, R.R., 2014. Distributed Model Predictive Control Made Easy. In: Intelligent Systems, Control and Automation: Science and Engineering, Volume 69. Springer, Dordrecht, The Netherlands.
J.M. Maestre, L. Raso, P.J. van Overloop, and B. De Schutter. Distributed tree-based model predictive control on an open water system. In Proceedings of the American Control Conference, pages 1985–1990, Montréal, Canada, June 2012.
J.M. Maestre P. Chanfreut and E.F. Camacho. Coalitional model predictive control on freeways traffic networks. IEEE Transactions on Intelligent Transportation Systems, May 2020.
R. Martí, S. Lucia, D. Sarabia, R. Paulen, S. Engell, and C. de Prada. An efficient distributed algorithm for multi-stage robust nonlinear predictive control. In Proceedings of the European Control Conference, pages 2664–2669, Linz, Austria, July 2015.
Mayne, D.Q., Kerrigan, E.C., van Wyk, E.J., Falugi, P., 2011. Tube-based robust nonlinear model predictive control. Int. J. Robust Nonlinear Control 21 (11), 1341–1353.
C. Menelaou, S. Timotheou, P. Kolios, and C.G. Panayiotou. Joint route guidance and demand management for multi-region traffic networks. In 2019 18th European Control Conference (ECC), pages 2183–2188, Naples, Italy, Italy, June 2019.
Messmer, A., Papageorgiou, M., 1990. METANET: A macroscopic simulation program for motorway networks. Traffic Engineering & Control 31 (9), 466–470.
Negenborn, R.R., De Schutter, B., Hellendoorn, J., 2008. Multi-agent model predictive control for transportation networks: Serial versus parallel schemes. Eng. Appl. Artif. Intell. 21 (3), 353–366.
Papamichail, I., Kotsialos, A., Margonis, I., Papageorgiou, M., June 2010. Coordinated ramp metering for freeway networks – A model-predictive hierarchical control approach. Transportation Research Part C: Emerging Technologies 18 (3), 311–331.
Pasquale, Cecilia, Sacone, Simona, Siri, Silvia, De Schutter, Bart, 2017. A multi-class model-based control scheme for reducing congestion and emissions in freeway networks by combining ramp metering and route guidance. Transp. Res. Part C 80, 384–408.
Pasquale, Cecilia, Sacone, Simona, Siri, Silvia, Ferrara, Antonella, 2019. Traffic control for freeway networks with sustainability-related objectives: Review and future challenges. Annual Reviews in Control 48, 312–324.
Piacentini, G., Goatin, P., Ferrara, A., 2018. Traffic control via moving bottleneck of coordinated vehicles. IFAC-PapersOnLine 51 (9), 13–18.
Precup, R.E., Hellendoorn, H., 2011. A survey on industrial applications of fuzzy control. Comput. Ind. 62 (3), 213–226.
Richards, A., How, J.P., 2007. Robust distributed model predictive control. Int. J. Control 80 (9), 1517–1531.
Schildbach, G., Fagiano, L., Frei, C., Morari, M., 2014. The scenario approach for stochastic model predictive control with bounds on closed-loop constraint violations. Automatica 50 (12), 3009–3018.
Scokaert, P.O.M., Rawlings, J.B., Meadows, E.S., 1997. Discrete-time stability with perturbations: Application to model predictive control. Automatica 33 (3), 463–470.
Sirmatel, I.I., Geroliminis, N., 2018. Economic model predictive control of large-scale urban road networks via perimeter control and regional route guidance. IEEE Trans. Intell. Transp. Syst. 19 (4), 1112–1121.
Srinivasan, D., Choy, M.C., Cheu, R.L., 2006. Neural networks for real-time traffic signal control. IEEE Trans. Intell. Transp. Syst. 7 (3), 261–272.
Tettamanti, T., Luspay, T., Kulcsár, B., Péni, T., Varga, I., 2014. Robust control for urban road traffic networks. IEEE Trans. Intell. Transp. Syst. 15 (1), 385–398.
Xie, Lei, Cai, Xing, Chen, Junghui, Hongye, Su., 2016. GA based decomposition of large scale distributed model predictive control systems. Control Engineering Practice 57, 111–125.
X. Zhang, G. Schildbach, D. Sturzenegger, and M. Morari. Scenario-based MPC for energy-efficient building climate control under weather and occupancy uncertainty. In Proceedings of the European Control Conference, pages 1029–1034, Zürich, Switzerland, July 2013.
Zheng, X., Recker, W., 2013. An adaptive control algorithm for traffic-actuated signals. Transportation Research Part C: Emerging Technologies 30, 93–115.